ENVIRONMENTAL CHARACTERIZATION OF GLOBAL SOURCES OF ATMOSPHERIC SOIL DUST IDENTIFIED WITH THE NIMBUS 7 TOTAL OZONE MAPPING SPECTROMETER (TOMS) ABSORBING AEROSOL PRODUCT

Joseph M. Prospero,[1] Paul Ginoux,[2] Omar Torres,[3]
Sharon E. Nicholson,[4] and Thomas E. Gill[5]

Received 8 December 2000; revised 19 September 2001; accepted 8 November 2001; published 4 September 2002

[1] We use the Total Ozone Mapping Spectrometer (TOMS) sensor on the Nimbus 7 satellite to map the global distribution of major atmospheric dust sources with the goal of identifying common environmental characteristics. The largest and most persistent sources are located in the Northern Hemisphere, mainly in a broad "dust belt" that extends from the west coast of North Africa, over the Middle East, Central and South Asia, to China. There is remarkably little large-scale dust activity outside this region. In particular, the Southern Hemisphere is devoid of major dust activity. Dust sources, regardless of size or strength, can usually be associated with topographical lows located in arid regions with annual rainfall under 200–250 mm. Although the source regions themselves are arid or hyperarid, the action of water is evident from the presence of ephemeral streams, rivers, lakes, and playas. Most major sources have been intermittently flooded through the Quaternary as evidenced by deep alluvial deposits. Many sources are associated with areas where human impacts are well documented, e.g., the Caspian and Aral Seas, Tigris-Euphrates River Basin, southwestern North America, and the loess lands in China. Nonetheless, the largest and most active sources are located in truly remote areas where there is little or no human activity. Thus, on a global scale, dust mobilization appears to be dominated by natural sources. Dust activity is extremely sensitive to many environmental parameters. The identification of major sources will enable us to focus on critical regions and to characterize emission rates in response to environmental conditions. With such knowledge we will be better able to improve global dust models and to assess the effects of climate change on emissions in the future. It will also facilitate the interpretation of the paleoclimate record based on dust contained in ocean sediments and ice cores. *INDEX TERMS:*0305 Atmospheric Composition and Structure: Aerosols and particles (0345, 4801); 0322 Atmospheric Composition and Structure: Constituent sources and sinks; 1625 Global Change: Geomorphology and weathering (1824, 1886); 1640 Global Change: Remote sensing; *KEYWORDS:*mineral dust; aerosols; TOMS; remote sensing; soils

Citation: J. M. Prospero, P. Ginoux, O. Torres, S. E. Nicholson, and T. E. Gill, Environmental characterization of global sou7rces of atmospheric soil dust identified with the nimbus 7 total ozone mapping spectrometer (TOMS) absorbing aerosol product, *Rev. Geophys.*, *40*(1), 1002, doi:10.1029/2000RG000095, 2002.

1. INTRODUCTION

[2] There is increasing interest in the atmospheric transport of mineral dust. Mineral dust may play an important role in climate forcing by altering the radiation balance in the atmosphere through the scattering and absorption of radiation [*Tegen et al*., 1997; *Haywood and Boucher*, 2000; *Harrison et al*., 2001; *Sokolik et al*., 2001]. Mineral dust could also affect climate indirectly by affecting cloud nucleation and optical properties [*Levin et al*., 1996; *Wurzler et al*., 2000]. In addition, dust can serve as a reaction surface for reactive gas species in the atmosphere [*Dentener et al*., 1996] and for moderating photochemical processes [*Dickerson et al*., 1997]. Mineral dust is believed to play an important role in many marine biogeochemical processes. Trace metals on dust are essential to some marine biological processes.

[1]Rosenstiel School of Marine and Atmospheric Science, University of Miami, Miami, Florida, USA.
[2]Goddard Space Flight Center, Georgia Institute of Technology, Greenbelt, Maryland, USA.
[3]Joint Center for Earth Systems Technology, University of Maryland, Baltimore County, Baltimore, Maryland, USA.
[4]Department of Meteorology, Florida State University, Tallahassee, Florida, USA.
[5]Department of Civil Engineering and Department of Geosciences, Texas Tech University, Lubbock, Texas, USA.

8755-1209/02/2000RG000095*$15.00*
1002, doi:10.1029/2000RG000095

Dust is a source of Fe which in some ocean regions may be a limiting nutrient for phytoplankton [*Falkowski et al*., 1998; *Fung et al*., 2000]; consequently, dust could modulate the global carbon cycle. Moreover, certain species of cyanobacteria that utilize Fe in their metabolism could play a significant role in the nitrogen chemistry of the ocean; the rate of production of nitrate and ammonium by these organisms could be strongly controlled by the rate of input of mineral dust to the oceans [*Michaels et al*., 1996; *Falkowski et al*., 1998]. Dust also has an important role in paleoclimate studies. The concentration of windblown mineral dust in deep-sea sediments [*Rea*, 1994; *Kohfeld and Harrison*, 2001] and ice cores [*Yung et al*., 1996; *Kohfeld and Harrison*, 2001] is often used as a proxy indicator of paleoclimate aridity on the continents and of changes in the global wind systems.

[3] It is now well established that large quantities of mineral dust are carried over the oceans from arid continental regions around the world. Aerosol studies carried out over the past several decades have documented the temporal and spatial variability of dust transport over the oceans [*Duce*, 1995; *Prospero*, 1996a, 1996b; *Gao et al*., 2001]. Satellite imagery clearly shows that dust aerosols often cover very large ocean areas. Indeed, the values of aerosol optical thickness associated with dust transport are much greater than those attributed to pollution aerosols transported from sources in North America, Europe, and Asia; furthermore, the dust plumes cover much larger area, are more persistent, and occur more frequently than those associated with pollutant aerosols [*Husar et al*., 1997]

[4] While progress has been made in characterizing the importance of mineral dust in global-scale processes, there has been less progress in identifying the sources of large-scale dust, the environmental processes that affect dust generation in these source regions, and the meteorological factors that affect the subsequent transport. The anecdotal observations of travelers and the results of many field programs have identified specific types of environments that seem to be abundant sources of dust. Similarly, many studies have characterized dust generation on a micrometeorological scale [*Gillette*, 1981, 1999]. These have shown that dust mobilization is extremely sensitive to a wide range of factors, including the composition of the soils, their moisture content, the condition of the surface (especially the degree of disturbance), and wind velocity. Nonetheless, it has been difficult to place these observations into a larger context so that source regions could be identified on regional and global scales. While some satellite products have been useful in characterizing dust transport over the oceans [see, e.g., *Husar et al*., 1997; *Moulin et al*., 1998], they cannot be readily used to identify sources because of difficulties associated with the large temporal and spatial variability of the albedo of land surfaces. Techniques based on measurements of upwelling thermal (infrared) emissions [*Ackerman*, 1997], while useful, suffer from various difficulties including the effects of cloud and water vapor, so that it is difficult to detect coherent spatial patterns over dust source regions.

[5] It has recently been shown that the Total Ozone Mapping Spectrometer (TOMS) on the Nimbus 7 satellite yielded data that can be used to map the distribution of absorbing aerosols which are largely comprised of black carbon (i.e., soot), emitted primarily from biomass-burning regions, and mineral dust, most commonly emitted from sources in arid regions but also from occasional volcanic eruptions [*Herman et al*., 1997; *Torres et al*., 1998]. Because TOMS measurements are made in the ultraviolet (UV) spectrum and because the UV albedo of continental surfaces is low and relatively invariant, TOMS can readily detect absorbing aerosols over land surfaces as well as water. With TOMS one can clearly observe the occurrence of large dust events over the continents and subsequently follow the movement of large-scale plumes over the oceans [*Herman et al*., 1997]. While it is not possible to make an objective distinction between aerosol derived from biomass burning and that from dust sources, such a distinction can be made in a general way based on aerosol measurements made during past field campaigns and on a general knowledge of these regions (weather, climate, land use, agricultural practices, etc.) [see, e.g., *Husar et al*., 1997]. In addition, biomass burning is now closely monitored by a number of satellites.

[6] In this report we systematically examine the TOMS absorbing aerosol product over a 13-year period (1980–1992) for evidence of persistent dust sources. The TOMS data [*Herman et al*., 1997] show that on a global scale the dominant sources of mineral dust are all located in the Northern Hemisphere, mainly in North Africa, the Middle East, Central Asia, and the Indian subcontinent. TOMS also shows that there are large seasonal changes in dust distribution patterns and that these patterns often display a characteristic geometry. Although these patterns may change seasonally, sometimes disappearing during some seasons, they appear year after year. A cursory examination of maps reveals that the geometry of the TOMS aerosol distributions over specific regions can often be associated with geomorphological features, in particular, topographical lows in arid or semiarid regions.

[7] In this work we identify and characterize major dust source regions on the basis of the appearance of persistent spatial-temporal patterns in the TOMS aerosol distribution. We locate the patterns on maps and on topographical projections of land surfaces. This information coupled with knowledge of local environments enables us to identify those characteristics that are important for dust generation. In a related paper, *Ginoux et al*. [2001] present the results of a global dust model that incorporates the findings of this paper with regard to source environments.

2. DESCRIPTION OF THE TOMS ABSORBING AEROSOL PRODUCT

[8] The TOMS instrument flew on the Nimbus 7 polar-orbiting satellite from November 1978 to May 1993. TOMS provided daily coverage of most of the Earth's surface with a spatial resolution of 50 × 50 km at nadir and 150 × 250 km at extreme off nadir. The TOMS instrument was designed to provide global estimates of total column ozone using backscattered UV radiance measured in six bands (313, 318, 331, 340, 360, and 380 nm). Aerosol measurements are made in the three longest wavelengths (340, 360, and 380 nm), where gaseous absorption is weak and where the backscattered radiation is primarily controlled by molecular scattering, surface reflection, and scattering from aerosol and clouds. The TOMS aerosol algorithm is described in detail by *Herman et al*. [1997] and *Torres et al*. [1998]. Briefly, the radiative effect of aerosols is measured in terms of an aerosol index (AI):

$$\mathrm{AI} = -100 \log_{10}[(I_{340}/I_{380})_{\mathrm{meas}} - (I_{340}/I_{380})_{\mathrm{calc}}], \qquad (1)$$

where I_{meas} is the measured backscattered radiance at a given wavelength and I_{calc} is the radiance calculated at that wavelength using an atmospheric model that assumes a pure gaseous atmosphere. The difference between the measured and calculated radiances is attributed to aerosols. Nonabsorbing aerosols (e.g., sulfate aerosols and sea-salt particles) yield negative AI values. UV-absorbing aerosols (e.g., dust and smoke) yield positive AI values. Clouds yield near-zero values. In this paper we deal only with absorbing aerosols; henceforth, we refer to the positive values from (1) as the "absorbing aerosol index," the "AAI," or simply the "TOMS index." The TOMS AAI data used in this study have been reduced to a standard grid 1° latitude by 1.25° longitude. Ground-based studies in the tropical Atlantic show that mineral dust concentrations measured at the surface are highly correlated with TOMS AAI [*Chiapello et al*., 1999]; aerosol optical thickness measurements in dusty regions are also well correlated with TOMS AAI values [*Chiapello et al*., 1999; *Hsu et al*., 1999]. Current and archived TOMS aerosol products can be found at the NASA TOMS web site at http://toms.gsfc.nasa.gov/aerosols/aerosols.html. Monthly mean TOMS AAI visualizations for the period 1980 to present are available on the NASA's Earth Observatory web site at http://earthobservatory.nasa.gov/Observatory/Datasets/aerosol.toms.html. Here you can create various types of time series animations, including comparisons with other data sets (e.g., rainfall, vegetation, population, etc.).

3. CHARACTERIZATION OF DUST SOURCE REGIONS

3.1. Introduction

[9] The objective of this study was to identify relatively strong and persistent dust sources so as to be able to relate the dust to specific regions. To this end we worked primarily with daily TOMS AAI data to prepare maps showing monthly mean AAI frequency-of-occurrence (FOO) statistics for all 13 years of the Nimbus 7 TOMS record. TOMS AAI values typically range from near zero to as large as 5 (representing an extremely intense dust or smoke event). In order to eliminate minor dust events and to reduce the statistical "noise" introduced by low AAI readings, we used threshold filters that eliminated daily AAI data below a specified value. We visually inspected monthly mean AAI FOO products produced with thresholds ranging from 0.2 to 1.0 to assess which value yielded the most consistent patterns. Figure 1 shows the global FOO distribution of absorbing aerosol for January and July based on TOMS analysis of daily TOMS AAI values > 7 for the period 1980–1992. Figure 1 will be discussed in detail in section 3.3.1. At this time, it is sufficient to note the coherent distribution of absorbing aerosol and the large seasonal contrast.

[10] We also prepared monthly mean maps of TOMS AAI values. In our discussion we show some examples of

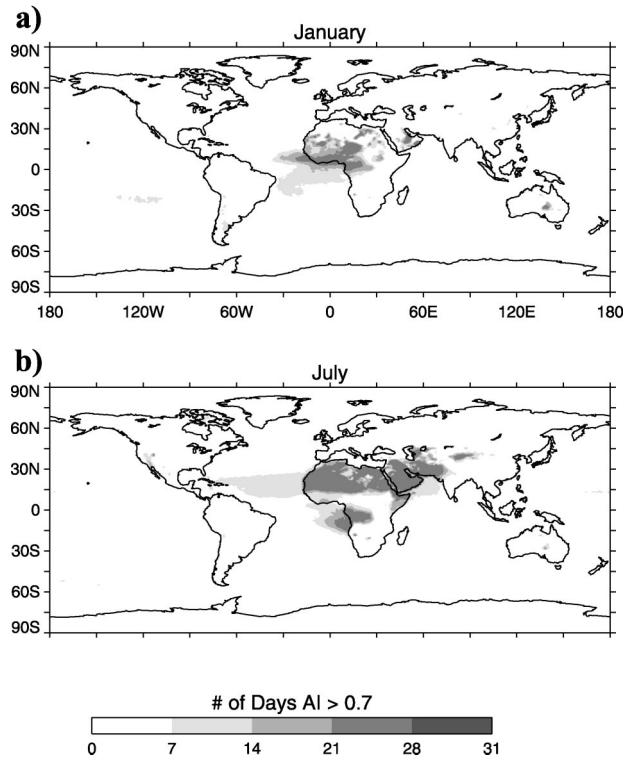

Figure 1. Global distributions of dust and smoke: monthly frequency of occurrence of TOMS absorbing aerosol product over the period 1980–1992. (a) January and (b) July. Scale is number of days per month when the absorbing aerosol index (AAI) equals or exceeds 0.7. In July the large dark area in southern Africa is due to biomass burning. In January, there is biomass burning in the region just north of the equator in Africa; part of the plume over the equatorial ocean is due to smoke. Essentially, all other distributions in Figure 1 are due to dust.

these distributions primarily to demonstrate that the two approaches yield similar results. However, we rely primarily on the FOO approach because the distributions are easier to interpret.

[11] There are several factors that complicate the interpretation of the TOMS AAI product. The detection of absorbing aerosols is based on the perturbation of the backscattered UV flux that originates below the aerosol layer. Because the albedo of land and water surfaces in the UV is typically only several percent [*Herman and Celarier*, 1997], essentially all of the UV upwelling flux originates from backscatter from the gaseous constituents in the atmosphere. Consequently, for any given total column aerosol concentration, aerosol at the top of the atmosphere will yield a larger value of the TOMS AAI than an equal amount of aerosol at a lower altitude. *Hsu et al*. [1999] show that the altitude dependence is linear. Thus TOMS is most sensitive to aerosol in the middle and upper troposphere and in the stratosphere; aerosols lofted to these altitudes are most likely to be carried over great distances. On the other hand, TOMS is least sensitive to aerosols in the boundary layer, where aerosol residence times are short. In fact, aerosols below ~500–1000 m are unlikely to be detected by TOMS [*Torres et al*., 1998, 2002]. This factor coupled with the use of thresholds in determining FOO distributions effectively eliminates low-altitude events. For these reasons and others [*Torres et al*., 1998] one cannot simply use mean AAI values to compare the relative strengths of dust sources in different climate and meteorological regimes; nonetheless, within specific regions and in specific seasons, the AAI should provide a rough measure of relative dust concentrations and hence relative source strength.

[12] TOMS can retrieve aerosol data in partially clouded pixels but not in regions covered with cloud except for aerosol above the cloud [*Herman et al*., 1997; *Torres et al*., 1998]. Because we use an AAI threshold filter followed by FOO analysis, our study is biased against dust source regions that are frequently covered with cloud and those that are only sporadically activated by relatively infrequent meteorological events. Some of these sources could conceivably play an important role in large-scale dust transport. Nonetheless, TOMS should yield relatively unbiased distributions over arid regions because of the relatively sparse cloud cover.

3.2. Global Distribution of TOMS AAI Values

3.2.1. Introduction

[13] The TOMS AAI FOO distributions in Figure 1 show that on a global scale the concentrations of absorbing aerosol are greatest in July and that the largest sources are located in the Northern Hemisphere. Essentially all the detected aerosol in Figure 1 is due to mineral dust. The major exception is the large area in southern Africa and the adjacent ocean in July; this feature is attributable to biomass burning [*Hao and Liu*, 1994]. Most notable in July is the huge dusty region that extends from the west coast of North Africa, through the Middle East, into Central Asia. A similar image in spring would show dust activity in China, extending almost to the Pacific Ocean. We henceforth refer to this region as the "global dust belt." In January (Figure 1a), there is much less dust activity in the dust belt. Biomass burning is also a factor. The prominent TOMS FOO feature along the coast of the Gulf of Guinea in North Africa is mostly attributable to biomass burning aerosol, but large amounts of dust are also present, transported from sources further inland [*Maenhaut et al*., 1996]. The over-ocean plumes in Figures 1a and 1b are also prominent in the advanced very high resolution radiometer (AVHRR) aerosol optical thickness product, which shows the same seasonal variability [*Husar et al*., 1997] seen here in TOMS.

[14] Outside the global dust belt, TOMS detects remarkably little large-scale, persistent dust activity. Nonetheless a number of sources are weakly seen in Figure 1. These include an area in the Great Basin in southwestern North America (July), a prominent area in Australia north of Lake Eyre (visible in January and also to a lesser extent in July), some weak sources in southern South America, especially in Argentina, and two small sources in southern Africa in July (to the south of the large area of biomass burning).

3.2.2. Dust Belt Annual and Interannual Trends

[15] There is a large temporal and spatial variability in dust emissions in the dust belt (Figure 2). In North Africa the maximum dust transport occurs in summer when large quantities of dust are carried across the Mediterranean to Europe and the Middle East [*Moulin et al*., 1998] and across the Atlantic to the Caribbean [*Prospero and Nees*, 1986], the southeastern United States [*Perry et al*., 1997; *Prospero*, 1999], and the mid-latitude western North Atlantic [*Arimoto et al*., 1995]. There is also considerable transport in the winter months when large quantities of dust are carried into South America [*Prospero et al*., 1981; *Swap et al*., 1992]. Dust activity is at a minimum in the fall.

[16] The locus of dust activity shifts with the season. In North Africa the winter dust activity is greatest in the low latitudes; as the year progresses, dust activity moves to the higher latitudes. In the Middle East, activity peaks in the late spring and summer and is at a minimum in the winter. Over the Indian subcontinent, activity peaks in the spring and decreases in the summer with the onset of the southeast monsoon. In Asia, dust activity peaks in the spring. The seasonal cycles of dust activity observed by TOMS are generally consistent with meteorological observations of dust events [*Goudie*, 1983; *Goudie and Middleton*, 1992; *Middleton et al*., 1986] as observed in North Africa [*Mbourou et al*., 1997], the Middle East, Southwest Asia, and the Indian subcontinent [*Middleton*, 1986a, 1986b, 1989; *Ackerman and Cox*, 1989], and Asia [*Middleton*, 1989, 1991; *Littmann*, 1991], although there

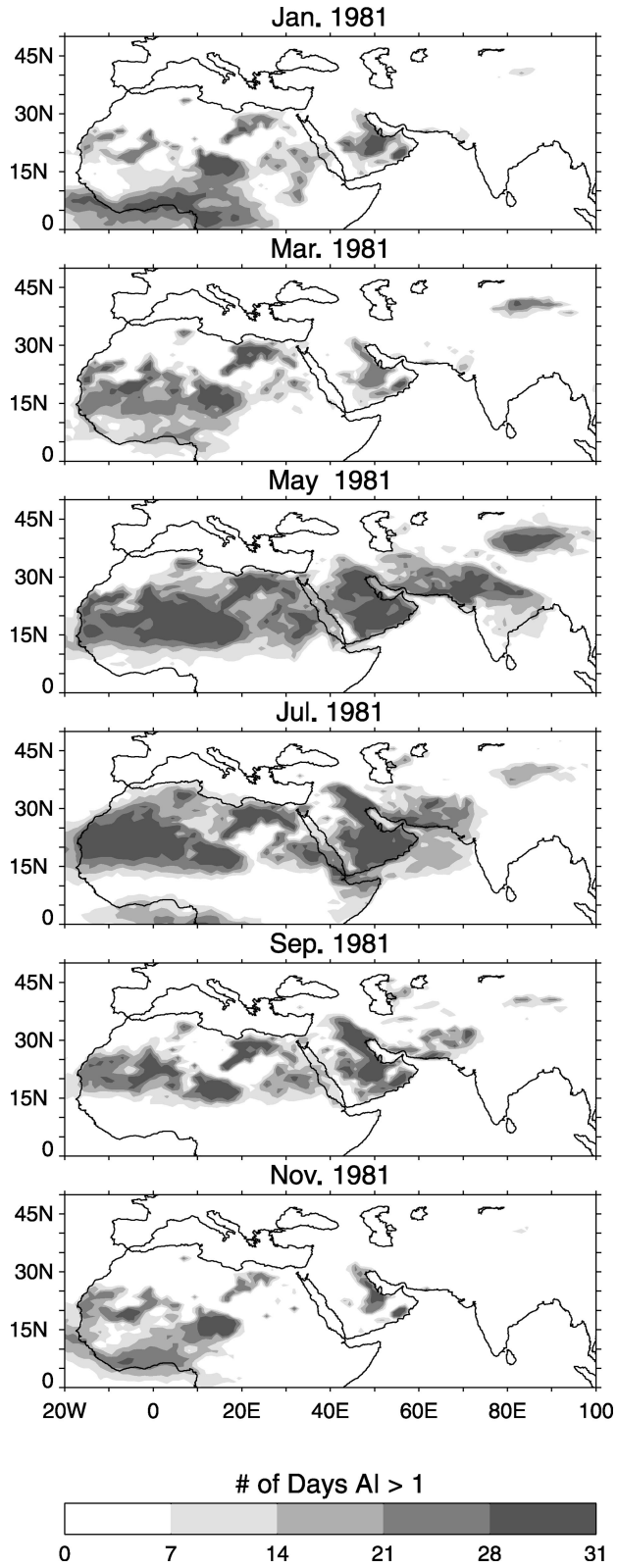

Figure 2. Seasonal variability of dust sources in the global dust belt. TOMS AAI frequency of occurrence (days per month when the AAI equals or exceeds 1.0) for the months of January, March, May, July, September, and November 1981. We use a threshold of 1.0 in order to suppress the almost constant background of blowing dust over much of this region.

can be substantial differences as in Australia [*McTainsh and Pitbaldo*, 1987].

[17] In Figure 2, one sees isolated source regions where the FOO values are relatively high and where the distributions assume a characteristic shape that persists from month to month. Some examples are, in North Africa, the spot near the Mediterranean in Tunisia and eastern Algeria (at about 34°N, 8°E), visible all year long; the elongated shape in eastern Libya (30°N, 20°E), also visible all year long; the long, narrow band near the west coast in Mauritania (25°N, 10°W), most clearly visible in January, March, May, and early and late in the year; areas on the Arabian Peninsula along the Persian Gulf and on the Arabian Sea; and the large area in central Asia (at ~40°N between 80° and 90°E) in March, May, and July. Most notable is a very large circular spot in the center of North Africa (centered at ~15°N, 15°E), active all year long. In many cases the FOO spots go through a cycle over a period of months; these patterns appear, grow in area and intensity, and then fade away. During this waxing and waning cycle one can often see within the larger dusty region small areas where FOO values are unusually high, which suggests that dust activity is particularly intense and persistent. These features are usually easiest to detect during seasons when dust activity is relatively low, and details of individual sources are relatively unobscured by heavy clouds of blowing dust. For example, in Figure 2, during the summer months much of West Africa is covered by heavy dust most of the time; here the activity of specific sources is best seen early in the year and late in the year. The persistence of these fixed points of intense dust activity suggests that conditions in these areas are particularly favorable for dust generation.

[18] The pattern of active spots and plumes is reproducible from year to year. Figure 3 shows the FOO product for the month of October for the years 1982 through 1987. This time span covers a period of extreme drought in North Africa that reached a peak in 1983–1984 [*Nicholson et al.*, 2000]. During 1983–1984, dust transport across the North Atlantic in the trade winds was the greatest ever observed since the start of measurements in 1965 [*Prospero and Nees*, 1986], a distinction that remains to this day [*Prospero*, 1996a]. The effects of the increased dust mobilization in North Africa in 1983–1984 can be seen in Figure 3. Nonetheless, the general geometric configuration of the active spots and the resulting plumes are relatively unchanged from year to year. This suggests that these sources are well established and that they are probably representative of longer-term conditions that affect dust generation.

3.3. Procedures and Sources Used in This Work

[19] Throughout this paper, we identify the location of active source regions and discuss the factors that might make them good sources of mineral dust. Our analyses are mostly based on FOO distributions as shown in the previous examples. In Figure 4 we show a

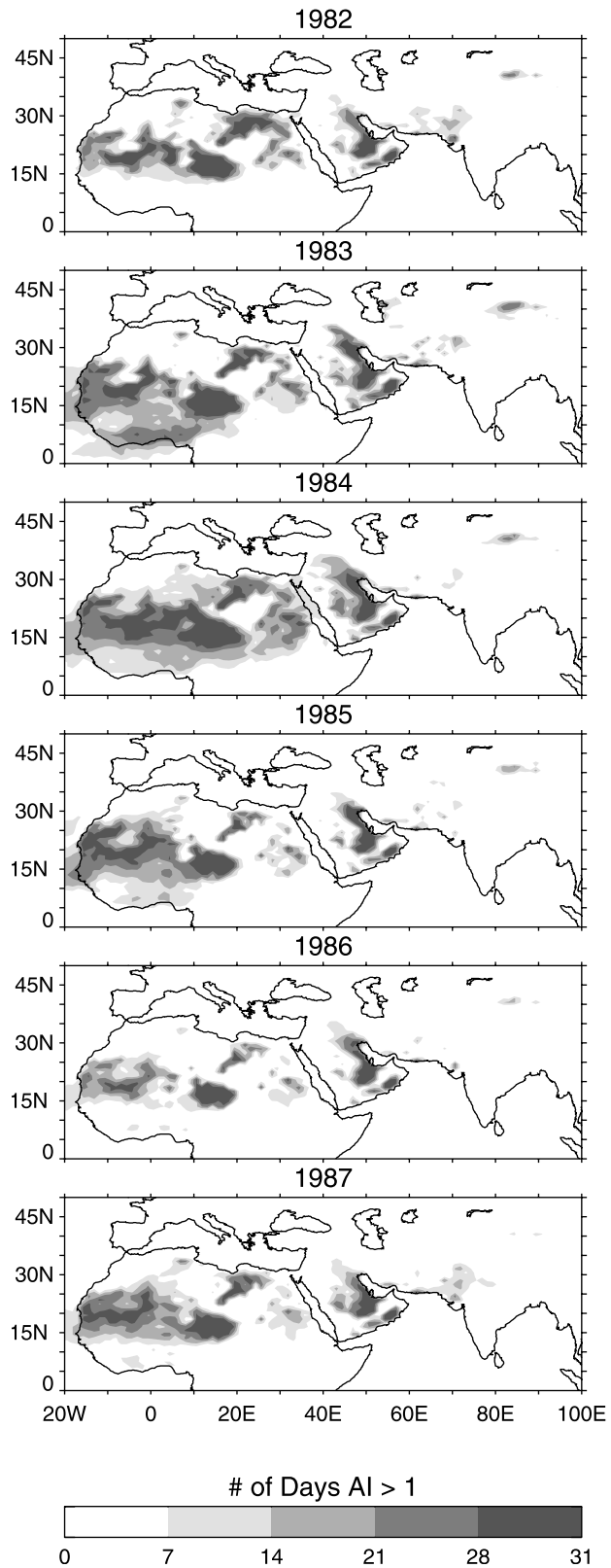

Figure 3. Interannual variability of dust sources in the global dust belt: TOMS AAI frequency of occurrence (days per month when the AAI equals or exceeds 1.0) in the global dust belt October 1982 through 1987.

composite of all major global dust sources identified in this work on the basis of FOO distributions. To prepare Figure 4, we selected for each source a specific month that best represents the long-term FOO distribution. Thus the configuration of sources shown in Figure 4 does not represent any specific season or year. Each of the sources shown in Figure 4 will be discussed in this paper.

[20] In addition, we processed the daily TOMS AAI data to obtain distributions of monthly and annual mean AAI values. We compare the FOO and AAI products with maps and atlases so as to identify the source regions and to characterize them in terms of geography and geomorphic features. For this purpose we used a wide variety of sources: Rand McNally *New Millennium Atlas* on compact disc [*Rand McNally*, 1998], the Rand McNally *Great Geographical Atlas* [*Rand McNally*, 1991], and the *Planet Earth Macmillan World Atlas* [*Macmillan*, 1997]. These were selected specifically because of their clear depiction of topography and geographical features. The Rand McNally compact disc atlas was especially useful because of the variable zoom factors, selectable level of details, and easy navigation with a latitude/longitude tool. We also used various map series specifically designed for travel and exploration in remote regions. These include maps from Michelin, Hallwag, Hildebrand, and RV Verlag. These maps provide a high level of detail on topography, terrain, and water features. In our discussion of the source regions we briefly and broadly review the major features of the geography and climate. For the most part, these are summarized from various general sources, in particular, the Encyclopaedia Britannica [*Encyclopaedia Britannica*, 2000] (hereinafter referred to as EB).

[21] We also used various visual satellite products in conjunction with this study. Sea-viewing Wide Field-of-view Sensor (SeaWiFS) images were particularly useful. These were obtained largely from the SeaWiFS Interactive Region Selection web site (http://seawifs.gsfc.nasa.gov/cgibrs/seawifs_subreg.pl), which provides 4-km resolution zoomable images on a day-to-day basis. The NASA web site, Visible Earth (http://www.visibleearth.nasa.gov/Atmosphere/Aerosols/), has an archive of images of spectacular aerosol events, most devoted to dust events, many of which are associated with sources discussed in this paper.

[22] In the course of our discussion of the TOMS data and the implied dust sources we cite selected aerosol studies that are relevant to our interpretation. We also cite publications that present studies of meteorological data relevant to dust mobilization, that is, the standard observations for blowing dust, haze, and severely restricted visibility. Such data have limitations. First of all, there are few, if any, meteorological stations in many of the regions that we identify as major source areas. Second, station reports are not necessarily representative of larger areas; indeed, stations are normally located close to urban areas or agricultural lands where soil distur-

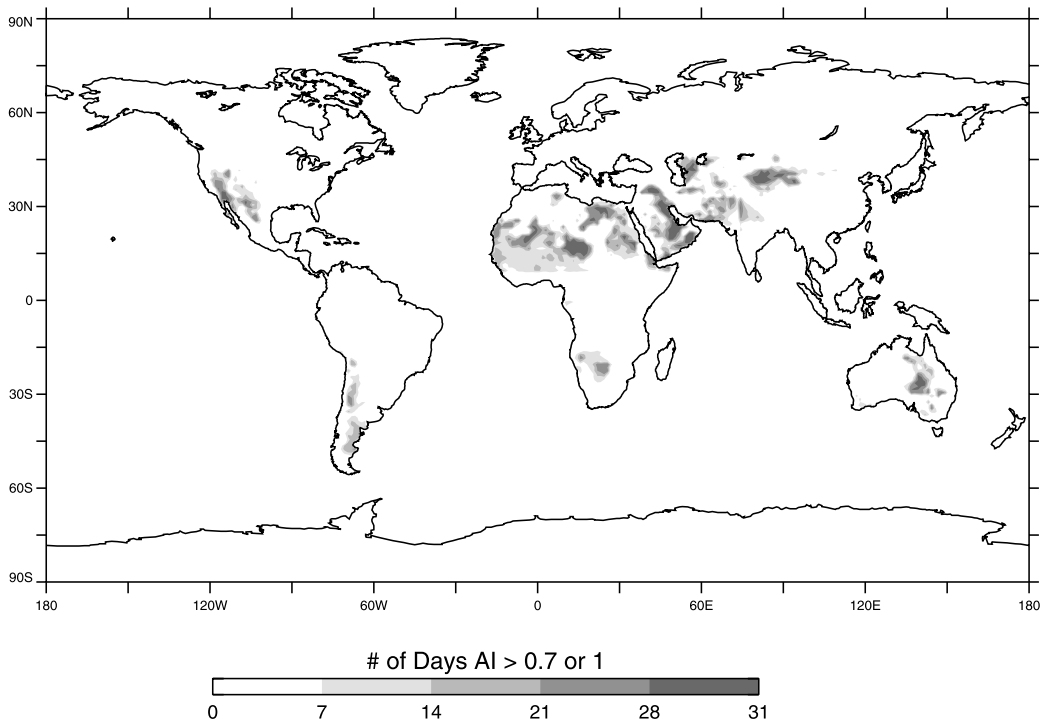

Figure 4. The global distribution of TOMS dust sources. Figure 4 is a composite of selected monthly mean TOMS AAI frequency of occurrence distributions for specific regions using those months which best illustrate the configuration of specific dust sources. The distributions were computed using a threshold of 1.0 in the dust belt and 0.7 everywhere else.

bances could lead to much increased dust activity on a local scale. Finally, such observations do not provide information about the depth of the dust layer, a factor that is relevant to long-range transport and also to the detectability of the dust by TOMS. Nonetheless, the degree of agreement or disagreement between such data and the TOMS reports provides some insight on these factors.

4. GLOBAL DUST BELT SOURCES

[23] The distribution of the TOMS dust sources is shown in Figure 5a, where representative monthly mean AAI FOO distributions are plotted on a topographic map. We used the 10-min resolution global elevation data set prepared by the Navy Fleet Numerical Oceanography Center at Monterey, California, and archived by the National Center for Atmospheric Research (NCAR) Data Support Section in Boulder, Colorado. For each 10×10 min area the set includes modal elevation, minimum and maximum elevation, terrain characteristics, and urban development. In our maps we show modal elevations and water bodies, salt lakes and dry lakes.

[24] Also shown in Figures 5b–5g are monthly mean AAI values for subregions in Figure 5a. A comparison of the mean AAI values with the AAI FOO values shows good agreement between the distributions of these two indices. Both data representations show that the most active TOMS dust sources are associated with topographic lows or they are situated in close proximity to mountains and highlands. In mountainous regions (e.g., Afghanistan, Iran, Pakistan, and China), strong dust sources are often found in closed intermountain basins. This close association of source with topographic lows is an important conclusion of our work and one that we will elaborate upon throughout this paper.

4.1. North Africa

4.1.1. Tunisia and Northeast Algeria

[25] There is a persistently active region located immediately to the south of the northern (Tell) Atlas Mountains (Figures 2, 3, 5a, and 5b). The greatest dust activity takes place near an extensive system of salt lakes and dry lakes found in the lowlands south of the Tell Atlas. The most intense and persistent activity occurs in the region immediately to the south of the salt lakes (called "chotts" here). The dusty region extends to the south and southeast, down to ~30°N, abutting the Atlas Mountains to the west. Maps show many ephemeral drainage channels from the Atlas to the lowlands to the east. *Quarmby et al*. [1989] described the region as a mixture of hillslope, channel, alluvial fan, and playa environments. *Rognon et al*. [1989] carried out a field program in this region and observed that the alluvial deposits associated with these channels were rich sources of dust; *Rebillard and Ballais* [1984] determined

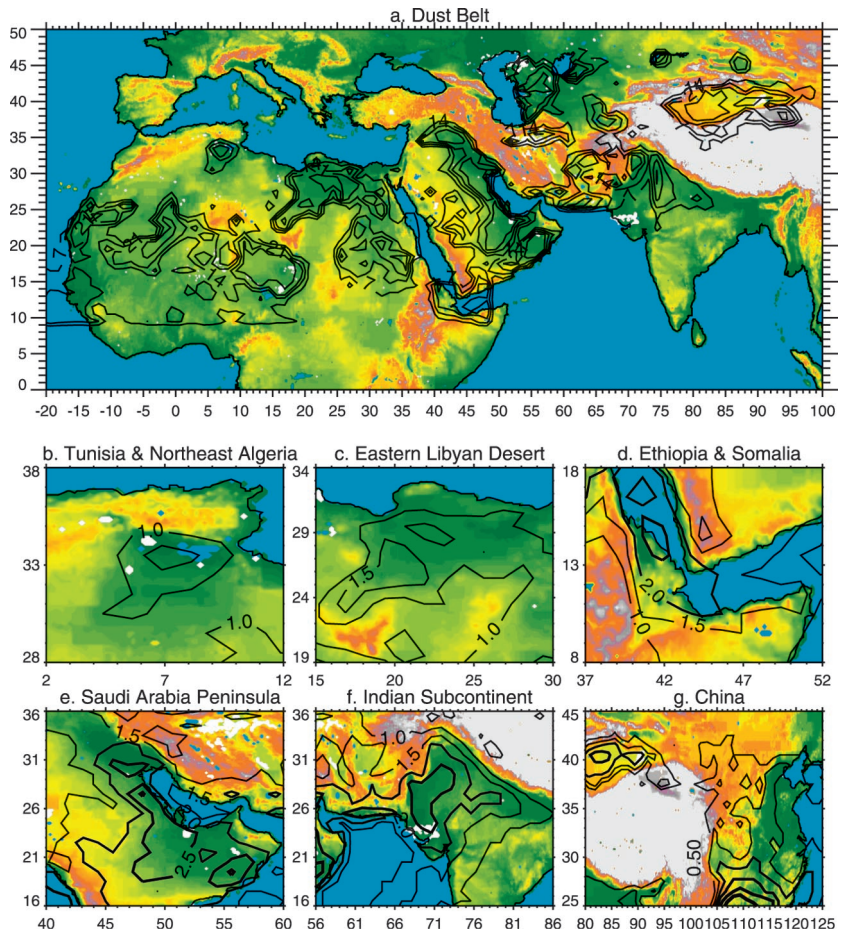

Figure 5. (a) Dust sources in the global dust belt and their association with topographic relief. Figure 5a is a composite made up of selected monthly mean TOMS AAI frequency of occurrence distributions (days per month when the AAI equals or exceeds 1.0) shown as isolines on a topographic map (10-min resolution data set from the Navy Fleet Numerical Oceanography Center, Monterey). Water bodies are in blue, and salt and dry lakes are shown as white. (b) Tunisia and eastern Algeria dust sources. Mean values of TOMS AAI, April 1986, are plotted as isolines on a topographic map. Two chotts (in blue) and associated dry lakes (in white) are located along 34°N at the base of the Tell Atlas. (c) Eastern Libya dust sources. Mean monthly values of TOMS AAI are plotted as isolines on a topographic map, March 1986. (d) Ethiopia and Eritrea dust sources. Mean monthly values of TOMS AAI are plotted as isolines on a topographic map, July 1986. The highest AAI values are centered slightly to the east of the Danakil Depression and the salt/dry lakes therein (white area). (e) Arabian Peninsula and Tigris-Euphrates dust sources. Mean monthly values of TOMS AAI are plotted as isolines on a topographic map, July 1990. (f) Indian subcontinent and Middle East dust sources. Mean monthly value of TOMS AAI are plotted as isolines on a topographic map, June 1991. (g) Asian dust sources. Mean monthly values of TOMS AAI are plotted as isolines on a topographic map.

that sand sheets and related aeolian features were found on the surfaces and edges of the chotts. The most intense activity starts in April–May and extends to August–September. The chotts and the associated dust source regions lie in the rain shadow of the Tell Atlas; they directly receive <100 mm of rain annually, and consequently, they normally have water only in the lowest areas. The largest are Chott Jerid (33.7°N, 8.4°E; 4900 km^2) in Tunisia and Chott Melrhir (34.3°N, 6.3°E; 1800 km^2) in northeastern Algeria. The most intense dust activity occurs in an area centered at 33.5°N, 7.5°E, between and to the south of these chotts (Figure 5b). The chotts are located in a depression that was formerly linked to the sea and which now extends 400 km westward from the Gulf of Gabes. To the south lies the Grand Erg Oriental (Great Eastern Erg), a vast sand sea (200,000 km^2) that extends 600 km to the southwest into central Algeria.

[26] Saline lakes, depressions, and dry lakes are part of a class of geomorphic features generally referred to as terminal lakes or playas. They are common features in many sources seen in TOMS, and in this paper we show that they serve as a good indicator of source environments. Playas are flat-bottomed depressions commonly found in interior desert basins and as "sabkhas" adjacent to coasts within arid and semiarid regions; in some

locations, these are periodically covered by water to form playa lakes, some of which are saline (EB). Ephemeral, salt, or dry lakes are referred to by many different names throughout the world: playas and playa lakes in North America; salinas, saladas, and salars in South America; chotts (shatts, shotts); sebkhas or sabkhas in the Middle East; boinkas in Australia; pans in southern Africa; nor, kavir, or gol in Asia [*Gill*, 1996]. In addition, a mixed descriptive terminology has informally evolved which further classifies the playa surface, particularly as to primarily evaporite (salt) covered or clastic (clay-silt) covered; aerosol-emitting playa surfaces themselves may vary widely over the course of a season [*Cahill et al*., 1996; *Gillette et al*., 2001]. A saline playa may be a salt flat, salt marsh, salt pan, or alkali flat; a salt-free playa may be termed a clay pan, hardpan, dry lake bed, or alkali flat. The diverse and confusing nomenclature for playas [*Rosen*, 1994] is not well standardized and is often contentious [*Briere*, 2000], reflecting the fact that they are a common feature all over the world and they are named according to local usage.

[27] Playas are often associated with large regions of deep alluvial deposits that were formed during pluvial periods. The accumulation of recent and ancient sediments in playas, often with salts which enhance the weathering of sediments, makes them good sources of fine-grained mineral particles [*Gill*, 1996; *Rognon et al*., 1989; *Reheis and Kihl*, 1995; *Middleton et al*., 1986; *Pye*, 1989; *Goudie and Wells*, 1995]. The association of playas and alluvial deposits with TOMS dust sources emphasizes the importance of the earlier climate history in the region in generating abundant quantities of mineral material that can be easily deflated by winds.

4.1.2. Eastern Libyan Desert

[28] A large area of dust activity extends over the eastern Libyan desert into western Egypt (Figures 2, 3, 5a, and 5c). These sources are active during much of the year. Activity is most intense in May–June. The northern part of this feature lies over a low-lying region that is marked with a number of drainage features, in particular, a chain of wadis (Wadi al-Farigh and Wadi al Hamim) which receive flow from the somewhat elevated coastal region to the north (the Al Jabar al Akhdar hill range in Libya, Figures 5a and 5c). The wadi system (and associated complexes of salt/dry lakes) extends from the Libyan coast on the Gulf of Sidra south of Banghazi (Benghazi) to the Qattara Depression (in Figures 5a and 5c, the white area near 30°N, 28°E). In this paper we will show that wadis (an ephemerally wet valley, gully, or streambed) are a common feature in many TOMS sources along with alluvial fans and playas. Indeed, these morphological features are often genetically linked to one another.

[29] The eastern extreme of the dust source is located over the southwestern end of the Qattara Depression. The active region extends in a relatively narrow corridor to the southwest to ~22°–23°N, 15°–17°E, bounded on the west by the Al-Haruj al-Aswad hill range (maximum altitude 1200 m) and the Jabal Bin Ghunaymah mountains and the Sarir Tibasti (Tibesti) highlands on the border with Chad.

4.1.3. Egypt

[30] The Egyptian sources become active in March and cease about October (Figures 2, 3, and 5a). The most active area is roughly oriented NW-SE with southeasternmost extension at ~24°–25°N, 33°E, a little north of Aswan, and the northwestern extension at ~27°N, 29°E. As the dust season progresses, the TOMS distribution extends to the northwest and merges with the previously described Libyan source in the southwest of the Qattara Depression. The eastern boundary of the dust activity is largely defined by the west bank of the Nile. The western limit is in the low lying area in central Egypt, which is the location of a series of north-south trending escarpments, depressions (Kharga, Dakhla, Farafra, and Bahariya), and associated oases and the only major road in the interior. The dust source lies over a region marked in some maps as the Gurd Abu Muharrik, which does not have any major dune systems [*Lancaster*, 1996, Figure 13.6]. In contrast, TOMS shows no major dust sources over the Great Sand Sea in the Western Desert.

[31] The Mediterranean is frequently impacted by dust storms in the late spring and summer [*Moulin et al*., 1998; *Guerzoni and Chester*, 1996; *Prospero*, 1996b]. The TOMS data suggest that the principal sources of the dust are most likely the regions described here in eastern Algeria, Tunisia, Libya, and Egypt.

4.1.4. Sudan and the Flanks of the Ethiopian Highlands

[32] Source identification is complicated in the south by widespread biomass burning (as identified by satellites) especially south of ~15°N from about October to March. During maximum dust activity in May–July, high AAI values extend from the western flanks of the Ethiopian highlands west to the plateaus of western Sudan and eastern Chad (Ennedi Plateau), roughly between 15° and 22°N (Figures 2, 3, and 5a) The southern extension of the dust area wraps around the Tilal an Nuba (Jibal an-Nubah), a region of highlands (maximum heights around 900–1300 m) that lies to the southwest of Khartum (15.5°N, 32.5°E). The Nile flows between these highlands. As the season progresses into the summer, the dust activity moves to the northeast along the flanks of the Ethiopian highlands, extending to the Red Sea. Within this larger dusty region, TOMS shows a number of particularly active sources. One is centered at ~18.5°N, 25.5°–26.0°E, immediately to the east of the Mourdi Depression on the northern flanks of the Ennedi Plateau. This appears to be the site of early Holocene paleolake Ptolemy, described by *Pachur* [1997] as an area where "at the present time, the lake sediments are undergoing deflation and groups of barchans (moving

sand dunes) are traversing the former lake basin." Another is at 18°N, 28°E, at the terminus of one of the largest wadis emanating from the Ennedi Plateau, Wadi Howar (Ouadi Howa). Two other sources are located between the Nile and the highlands (peaks ~1000–2200 m) to the east that flank the Red Sea. Especially active spots are centered at ~20°N, 32°E and at 18°N, 35°E; both are located in the Nubian Desert in regions where maps show very extensive ephemeral channels that extend from the highlands toward the Nile. The source at 18°N, 35°E includes Wadi Langeb, a pass to the south of Port Sudan. This wadi is the frequent source of spectacular dust storms. Satellite images (especially SeaWiFS) often show large, intense dust plumes jetting out of the wadi and over the Red Sea (at ~18.5°N, 38°E) [*Schroeder*, 1985]. The dust is generally swept to the south, passing through the narrow straits between Eritrea and Somalia to the west and Yemen to the east into the Gulf of Aden (see section 4.1.5).

4.1.5. Ethiopia Rift Valley and Djibouti

[33] Dust activity in this region peaks in June and July. There is little activity during the remainder of the year (Figure 2). Dust distributions are sharply defined by the mountains to the west and to the south in Ethiopia, Eritrea, and Somalia and to the east, across the Red Sea and the Gulf of Aden, the mountains in Yemen. In Ethiopia and Somalia the highlands (~4000 m high to the west and ~3000 m to the south) form a sharply defined right angle, which is clearly visible in the TOMS FOO and AAI distribution. In Figure 5d, TOMS shows a maximum at ~14°N, 42°E, slightly to the east of the Danakil Depression and Kobar Sink in the Rift Valley of northern Ethiopia and Eritrea. The Danakil receives runoff from the highlands to the east and west of the valley. There are extensive ephemeral drainage features along the eastern flanks of the Ethiopian highlands, including many swamps and marshes. Toward the northern end of the Danakil at l4°N, 40°E is an intermittent lake, Asake (area of 308 km^2). The location of the maximum AAI values in Figure 5d suggests that much of the dust activity is centered over and around this lake basin.

4.1.6. Mauritania and Western Sahara

[34] A series of sources lie near the west coast of North Africa starting to the west of the town of Nouadibou at ~21°N, 16°W and extending to the north through western Sahara and to the northeast through Mauritania to ~26°–27°N, 6°–7°W on the border with Algeria (Figures 2, 3, and 5a,). These are best seen in the FOO distributions early in the year, from January to May, and late in the year; during the intervening months these sources are obscured by the dense dust plume that covers this region [*Middleton*, 1989] and much of North Africa (see Figure 1a and Figure 2, May and July plots). The sources closest to the coast lie on the western slopes of the Adrar Souttouf, a modest highland that runs parallel to the coast. The more inland portion of the active area lies to the east of this highland. The elevations are for the most part only a few hundred meters (highest ~600 m), but maps show well-defined drainage systems emanating from these highlands. On the eastern side, where the dust activity is seen, there are many small (and a few quite large) water features and many playas. *Cornet* [1990] described the region as part of a "considerable" late Pleistocene stream and wetland system which would have caused lacustrine sediments to be dispersed over the area. The SW-NE alignment of the TOMS AAI distribution matches the distribution of these water features. It is notable that this source region lies on the northern and western edges of some huge sand seas (ergs). To the south is the Majabat al Koubra; to the east are Erg Iguidi and Erg Chech, both prominent on maps [*Lancaster*, 1996, Figure 13.2], which extend from the coast of Mauritania deep into Algeria. It is significant that early in the year the dust comes from the "wet" region, not from the erg system.

4.1.7. Mali, Mauritania, and the Western Flanks of the Ahaggar Mountains

[35] There is a complex distribution of dust sources located throughout this region. During the summer they are completely obscured by blowing dust. Consequently, we can only comment on dust activity during the low dust activity periods: from January to March and also late in the year, October–December (Figure 1a and Figure 2, January, March, and November plots). A large active area extends from ~17°–18°N, 8°–10°W to the ENE to ~26°N along the meridian. This vast region is poorly characterized, and maps (Michelin 953) show it to be virtually uninhabited; it has extensive dune systems. The area of maximum mean AAI values lies well to the north of the Niger River, although a small portion of the active area intersects the river at ~16°N, 3°–4°W, in the region of Tombouctou. There is one area in particular between 18° and 20°N and 3° and 8°W, northwest of Tombouctou, that appears to be a particularly active source all year long. Maps show no distinctive features in this region and no towns, villages, or roads of any kind.

[36] The shape of the TOMS FOO distribution (Figure 5a) is defined on the east by the 500–1000 m elevation line of the Ahaggar Mountains and on the south by an arm of the mountains that projects to the southwest and terminates in the Adrar des Ifoghas (Adrar des Iforas). The northern end of these sources terminates over a low-lying region centered at 26°N, 1°E on the northern end of the Tanezrouft in southern Algeria. This region receives extensive drainage from the Ahaggar; two large intermittent playas are located here (Azzel Matti and Meqerghane). *Chorowicz and Fabre* [1997] indicate that the system of braided streams and wadis moving alluvial deposits from the western flanks of the Ahaggar to these depressions was active in the Holocene.

4.1.8. Niger and the Southern Flanks of the Ahaggar Mountains

[37] A well-defined array of sources lies between 18° and 23°N, 3° and 6°E. (Figures 2, March and September plots, 3, and 5a). The geometry of this feature is defined by the Adrar des Ifoghas to the west, the Ahaggar to the north, and the Massif de l'Air (Air ou Azbine) to the east. The most persistently active source within this region is a low-lying area nested between the mountain slopes. Michelin map 953 and World Cart 651.33210 shows a huge system of ephemeral rivers and streams that largely drain the Massif de l'Air; the flow follows the Vallée de Azaouagh and eventually feeds into the Niger. This drainage system is by far the largest emerging from the Ahaggar massif, and it is the most prominent in all of North Africa (as shown on maps). As the dust season progresses, dust activity extends from this source to the northwest, across the Adrar Des Ifoghas (500–1000 m), linking with the sources on the western flanks of the Ahaggar and on the Tanezrouft.

4.1.9. Lake Chad Basin and the Bodele Depression

[38] This region is undoubtedly the most intense dust source in the world. Large areas of the basin are filled with dust (Figure 3) all year long (Figure 6). This is in agreement with visibility data from meteorological stations in the region [*Mbourou et al*., 1997], which show a high frequency of visibility reduction during all seasons except fall, when the rate decreases somewhat. The mean TOMS AAI values are the highest of any region in terms of both the monthly and annual means. The geometry of the active area matches that of the 500 m isoline of the Massif de l'Air (maximum altitude of 2022 m) to the west, the Tibesti massif (highest peak, Emi Koussi, 3415 m) to the north, and the Ennedi Plateau (highest point, Basso, 1450 m) to the east in western Chad and eastern Sudan. The southern boundary of the AAI distribution lies along the northern side of Lake Chad.

[39] Within this larger area, there is a particularly intense source that stands out clearly (Figure 6) and remains fixed all year long. The core of activity, based on the AAI 3.0 annual mean isoline, lies between 16° and 18°N and extends from 15° to 19°E. This places the source directly over the Bodele Depression and the Erg du Djourab; indeed, the very highest value of mean AAI (3.5) is located precisely over the lowest part of the depression. *Adetunji et al*. [1979] first identified this region as the likely source area of Harmattan dust haze. There is a second intense source farther to the west yielding monthly mean AAI maxima of 3.0 in April and July (Figure 6) centered at ~17.5°N between 12° and 14°E, on the southern edge of the Grand Erg du Bilma in northern Niger. *Volkel and Grunert* [1990] and *Grunert et al*. [1991] described early Holocene freshwater lakes in the Erg of Bilma, followed by several episodes of accumulation, weathering, soil formation, and aeolian mobilization of both sandy and lacustrine sediments on this

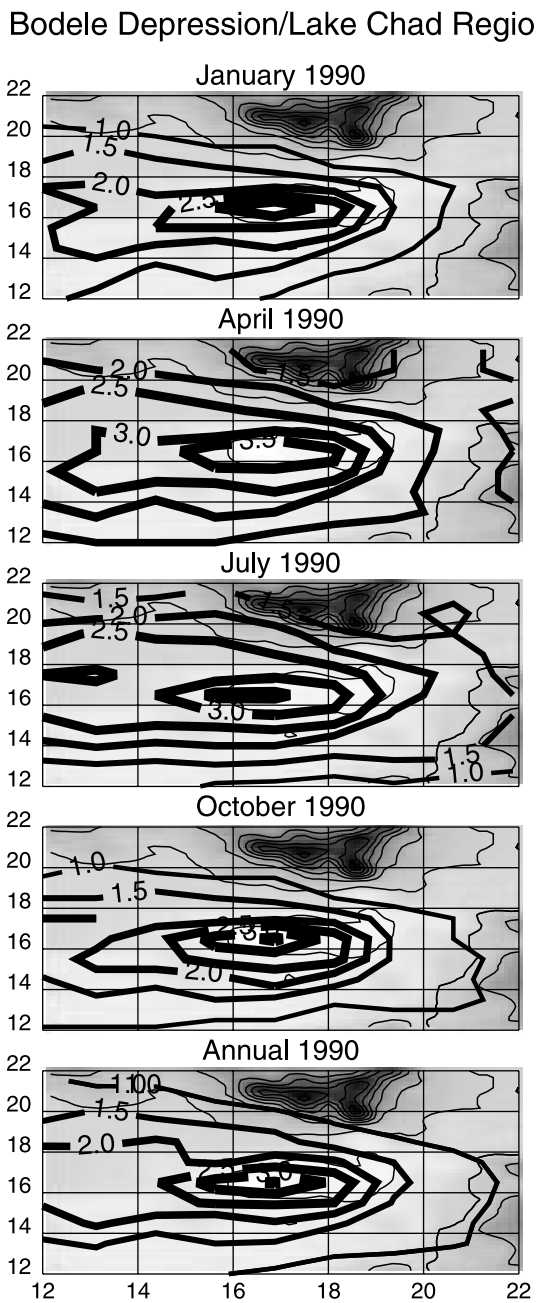

Figure 6. Chad and Niger dust sources: the Bodele Depression. Mean monthly values of TOMS AAI for 1990 are plotted as isolines on a topographic map (gray scale). The high elevations (dark shading) at the top of the plots are the Tibesti Mountains; on the right is the Ennedi Plateau.

southern side of the erg. *Goudie* [1983] identifies the region as an important source of dust that is transported south during the winter Harmattan.

[40] The Bilma and Bodele sources are located in extremely remote and desolate regions almost devoid of human habitation. The largest town associated with the Bodele source is Faya Largeau, located just to the north of the depression (at 17.9°N, 19.1°E); although it is a regional administrative center, it only has a population of 9000. The largest town associated with the intense

spot in Niger is Bilma (18.7°N, 12.9°E), with a population of 2400. There is considerable evidence (anecdotal, field measurements, and meteorological) that this region has been an extremely productive dust source since the time of the earliest explorations [*Kalu*, 1979; *McTainsh and Walker*, 1982; *Goudie*, 1983]. This region has a long recorded history because it was on the trans-Saharan trade route between West Africa and present-day Libya and on the Islamic pilgrimage route from West Africa to Mecca (EB). Travelers have long commented on the extremely intense dust activity in the region of Bilma and Faya Largeau.

[41] Maps provide no indications of particular features that might be associated with the source in the Bodele Depression. In satellite imagery (in particular, SeaWiFS), dust from this source is repeatedly (and often dramatically) visible during much of the year. Moreover, one can often see that the overall plume (which is typically hundreds of kilometers long) is comprised of many individual plumes that originate from sharply defined "point" sources. The persistence of this source region and the plume-like character of the individual sources within it shows how extremely sensitive dust production is to specific terrain and meteorological and environmental factors.

[42] Present-day Lake Chad lies in the southern end of this large drainage basin. In earlier times (most recently, during the last pluvial at ~6–8 ka), Lake Chad was quite large (EB), covering an area that is roughly comparable in size to the area of present-day intense dust activity. As a result, the basin is covered with a complex variety of sandy sediments, saline playas with evaporites [*Eugster and Maglione*, 1979], and thick, relatively fine grained lacustrine deposits which interact to serve as a rich source of dust. *Servant and Servant* [1970] first described how dune sands from the Erg du Djourab migrating across the dried lacustrine sediments of the Bodele Depression were responsible for actively generating the dusts of the Harmattan, and *McTainsh and Walker* [1982] pointed out how aerosol emission rates in the region are increased by wind-erodible salts atop the lake sediments [*Gill*, 1996].

[43] Maps show considerable drainage from the Tibesti into the Bodele and Faya Largeau regions; most drainage is carried by ephemeral rivers and streams that terminate in wadis and playas. In recent decades, Lake Chad has continued to be prone to dramatic water level fluctuations in response to short-term climate and land use factors [*Coe and Foley*, 2001].

[44] During the winter months the Bodele region is believed to be the major source of dust that is carried in the Harmattan to the Gulf of Guinea [*Kalu*, 1979; *Adetunji et al*., 1979; *McTainsh and Walker*, 1982] and subsequently across the Atlantic to South America [*Prospero et al*., 1981; *Swap et al*., 1992]. The transport path can be discerned in Figures 1a and 2 (January and December plots) as a plume extending from the Lake Chad Basin to the southwest, consistent with the cartoon depiction of dust transport from this region [*Kalu*, 1979] which is based on case studies and anecdotal evidence. The dust is not to be confused with the biomass burning that goes on along the Gulf coast in November–January where smoke is seen in Figure 2 as an elongated high FOO region oriented east-west just north of the equator and extending from central Africa to the central tropical North Atlantic. The smoke region is distinctly separated from the high TOMS values over the Lake Chad Basin. In Figure 2 the dust plume is seen as the lower toned (smaller FOO values) plume bridging the two regions.

4.1.10. Discussion: North African Sources

[45] There have been many efforts in the past to identify dust sources in North Africa using various types of field and meteorological observations [*Herrmann et al*., 1999]. These have resulted in a confused and conflicted picture which suggests that essentially all of North Africa could serve as a source [*Middleton and Goudie*, 2001], which in the broadest sense, is probably true. In contrast, TOMS shows that there are dominant sources and that these present a remarkably consistent pattern both from the standpoint of the geometry of the individual sources and the seasonal changes in their shape and distribution.

[46] Most of the prominent sources identified in Figures 2, 3, and 5 are associated with topographical lows or with regions on the flanks of topographical highs. In the latter regard, the Ahaggar and Tibesti Mountains dominate the sources in central North Africa. These mountains are ringed with some of the most active dust sources in North Africa and, indeed, the world. This suggests that weathering processes and runoff from the mountains play an important role in providing fine soil material that can be mobilized as dust.

[47] One of the striking aspects of the TOMS AAI distributions is that they are all located north of ~15°N. This is most clearly seen in Figures 2 (in May, July, and September plots) and 3. The southern boundary of the September–October distributions (when dust transport is approaching a minimum and before biomass burning becomes widespread) closely follows the 200–250 mm isohyet of rainfall [*Mortimore*, 1998, Figure 2.1, p. 10]. Similarly, in the north the only places where rainfall exceeds 200–250 mm is on the northern (Tell) Atlas and along the Mediterranean coast. Thus we conclude that in a broad regional sense, we should not expect to see strong dust sources in regions where rainfall is >200–250 mm. We reach the same conclusion throughout this paper in the analysis of the dust sources in other regions.

[48] In general, we do not see evidence that the major dune systems and sand seas are persistent sources of dust, although they may be important sources on a sporadic basis. For example, the Erg Chech in southern Algeria and Mauritania, one of the largest sand seas in the world, is not a persistent source (as defined by TOMS); the Great Sand Sea in the Western Desert of Egypt is similar. On the other hand, many of the most

active sources are located on the edges of these dune systems, a fact that may be linked to the mechanism of dust generation (see section 6.1). Often it is difficult to draw a clear distinction between the dust sources and the dune fields. For example, the core of activity in the Lake Chad basin lies over the Bodele Depression, which itself lies in close association with Erg du Djourab, a major sand sea.

[49] Finally, we have noted that many of the intense sources are associated with regions where there are extensive alluvial deposits. These sediments are either discharged through alluvial fans or wadis emanating from proximate highlands or deposited in recent pluvials. In this regard, it should be noted that TOMS does not see strong dust activity associated with the Niger River system and its associated sedimentary deposits. The Niger is located south of the 15°N and the 250 mm isohyet line except for a relatively small section of the river, which reached to ~17°N near Tombouctou (where, as noted above, major dust sources are seen). Thus, despite the rich source of particles in the river sediments, it appears that the environment is not now sufficiently arid for these soils to erode readily. If climate change brings increased aridity to this region, the Niger could become a rich source of dust.

4.2. Middle East

4.2.1. Arabian Peninsula

[50] Dust activity is visible over much of the peninsula all year long (Figure 2). Activity is low during the winter, grows strong in March–April, and increases to a maximum in June and July when much of the peninsula is covered with dust. The dust maximum observed by TOMS matches the monthly occurrence of dust storms as reported by meteorological stations [*Middleton*, 1986a; *Ackerman and Cox*, 1989]. There are two well-defined active areas, most clearly seen in the winter, spring, and fall (Figures 2, 3, and 5a). One extends along the eastern side of the peninsula along the Persian Gulf, and a second is near the coast in Oman. These two regions also stand out in both the TOMS AAI FOO (Figure 5a) and the monthly mean AAI (Figure 5e).

[51] The low-lying (50–200 m) flat terrain that borders the Persian Gulf is active all year long. This region has no prominent morphological features (e.g., sand fields, large wadis, etc). It is a geologically recent tidal flat, wider in the south and southwest (up to ~ 30 km wide), covered by sandy calcareous sediments and evaporites, the classic coastal sabkha [*Evans et al*., 1964; *Satchell et al*., 1981; *El-Sayed*, 1999]. In contrast to the other dust sources that we have identified thus far, most of the sediments originated from in situ or coastal processes not from fluvial deposits carried from higher elevations [*Evans et al*., 1964]. As the year progresses, the area of intense activity spreads to the south and then to the southwest over the Empty Quarter, the Rub' al-Khali. The configuration of the dust activity broadly reflects the geography of the region, a peninsula dominated by a high plateau (altitudes of ~1.5–3 km) that borders the Red Sea and slopes down toward the Persian Gulf. The western boundary of the active dust sources roughly conforms to the 200–500 m contour of the western plateau. It is notable that the plateau is rimmed by a borderland of sand sea, the Ad Dahna, which is 1300 km long; there is no indication of major dust activity in this region or in the sand sea farther west and northwest on the plateau, the An Nafud (area of 56,000 km^2).

4.2.2. Oman

[52] There are intense and clearly defined sources in Oman that are active all year long. Activity is greatest in June and July and weakest from November to February. Nonetheless, persistent sources are visible even in the low season when the spots are most readily identified in TOMS (Figures 2, January and November plots, and 3, October plot). These show the active region extending from the coast between ~54° and 58°E to ~200 km inland. The dust area is well delineated by the 200-m contour. To the northeast are the Al-Hajar Mountains, which lie parallel to the coast of the Gulf of Oman (altitudes of 1500–3000 m). This upland region is heavily dissected by deep wadis, which remain dry throughout most of the year but which flood after winter storms (EB). To the southeast lie the Jabal Dhofar (Zufar) mountains, which extend into Yemen (elevations to 1500 m). Southern Oman, especially the mountains, receives considerable moisture from the summer monsoon. The dust source region receives much drainage from these higher elevations (and, in the south, directly from the monsoon itself) (EB). Maps [*Hildebrand's Travel Map*, 1996] show the entire area laced with ephemeral drainage channels and wadis. The center of the most active area is located at 19°N, 56°E, but maps do not reveal any unusual features in this region. It is notable that dust activity is very strong even during the monsoon, which at lower elevations brings only ~10 cm of rain to the south (EB).

4.2.3. Tigris and Euphrates Basin

[53] Dust activity in the Tigris-Euphrates basin begins about May, reaches a maximum in July, and is much reduced by September-November (Figure 2), although there is considerable year-to-year variability. Activity starts in the southern reaches of the basin in the spring and spreads northward as the season progresses (Figures 2). The TOMS dust maximum coincides with that of dust storm reports from meteorological stations [*Middleton*, 1986a, 1986b]. During this season the region is dominated by northwesterly Shamal winds, which according to *Middleton* [1986a, 1986b], raise dust from the lower Tigris-Euphrates basin and carry it down the Arabian Gulf.

[54] At its maximum in July the geometry of the dust activity in TOMS is defined to the east by the Kabir Kuh

and Kuhha-ye Zagros mountain ranges in Iran. The curved shape of the FOO distributions to the north (Figures 2 and 3, July plot) conforms to mountains in southern Turkey. On the west is the Al Hamad Plateau of Saudi Arabia with elevations to ~1000 m; the geometry of the TOMS FOO distribution over this region conforms to elevation contours less than several hundred meters. The most intense dust activity occurs south of ~32°N, 200 km southeast of Baghdad. These sources are set in a vast alluvial plain that extends southward from 100 km north of Baghdad to the Persian Gulf (EB). These deposits cover >130,000 km^2; they have a uniformly low elevation, 100 m, and natural drainage is poor. Summers (May–October) are hot and arid, consistent with the maximum in dust activity observed by TOMS. Rains (100–180 mm annually) come to these lowlands in the winter. There is widespread seasonal flooding and extensive marshlands, some of which dry up in the summer to become salty wastelands. There is heavy soil erosion in much of Iraq, some of it induced by overgrazing and deforestation (EB). The river system has created at its mouth a large alluvial deposit that dates from Babylonian times. All these features appear to be rich sources of dust. In this context it should be noted that the core of dust activity is located at the southern end of the lowlands, centered at ~30°N, 45.5°–48.5°E. *Middleton* [1986b] reports an extremely high frequency of dust storms in this region, 43 per year at Abadan, making it one of the dustiest places in southwest Asia. This lies over the Al Basrah region in Iraq and the northern part of Kuwait. There do not appear to be any distinctive features in this region that would lead to greatly enhanced dust emissions. EB states that dust storms are frequent in the Mesopotamian plain and that the dust consists of "fine particles of clay and silt . . . which are from a remnant dune belt that has been formed from abandoned irrigated fields and dried-up marshes in the area between the two rivers. Only occasionally are there true sandstorms, bearing material from the western desert."

[55] It should be noted that there are vast desert regions (166,000 km^2) in western and southern Iraq, covering 40% of the country. The western desert has elevations to >500 m. The southern desert (elevations of 100–400 m) has a complex topography of rocky desert, wadis, ridges, and depressions. Yet TOMS does not show any substantial dust activity in these regions.

4.2.4. Discussion: Middle Eastern Sources

[56] The sources in this region extend in a continuous band from the upper reaches of the Tigris-Euphrates basin to the coast of Oman. Almost all major sources are located in low-lying terrains, typically below 200-m elevation. The major exception is the massive source in the Empty Quarter, one of the world's largest sand seas. In Iraq and Saudi Arabia, the sources appear to be associated with old alluvial deposits and with coastal sabkhas in the United Arab Emirates. It should be noted that the dust sources that we identify in Iraq lie in the "fertile crescent," the region where humans first began to practice systematic and widespread agriculture ~10,000 years ago [*Lev-Yadun et al*., 2000]. Indeed, the shape of the crescent can be clearly seen in the FOO distributions in Figures 2 and 5a. The alluvial deposits that were responsible for the fertility of this region when the climate was wetter are now the rich source of dust that we see today. In Oman, present-day fluvial action seems to play a major role in providing dust source material. The fact that the distribution and seasonality of dust as observed by TOMS agrees in a general way with the reports from meteorological stations [*Middleton*, 1986a, 1986b; *Ackerman and Cox*, 1989] suggests that most dust events are consistently associated with meteorological conditions that carry dust to moderately high altitudes. Various aerosol studies in the Arabian Sea confirm that very large concentrations of dust are carried to this region during the spring and early summer [*Savoie et al*., 1987; *Tindale and Pease*, 1999; *Satheesh et al*., 1999].

4.3. Central and South Asia

4.3.1. Caspian Sea and Aral Sea Region

[57] There is persistent dust activity in the region between the Caspian and Aral Seas. Activity generally starts in May and extends through August with the peak in June and July, but activity can occur sporadically all year long. Two plumes are prominent in FOO distributions (Figures 1b, 4, and 5a). The largest borders the east shore of the Caspian and extends to the Aral Sea. The most intense activity centered over the Garabogazköl (Kara-Bogaz Gol, "gol," playa or salt lake [*Gill*, 1996]; 41.3°N, 53.5°E), a large (9600 km^2) lagoon-like embayment which formerly was a gulf of the Caspian but was isolated from the sea by a man-made embankment during the years 1980–1992 and dried into a salt-covered playa [*Varushchenko et al*., 2000]. The embayment is surrounded by lowlands that are shown to be largely covered with swamps or marsh which are seasonally dry (EB). Several deflation basins are identified in this region [*Goudie and Wells*, 1995]. Persistent dust activity is also seen on the south and southeast end of the Aral Sea (44.3°N, 60.8°E) in the Turan Lowlands; Takhiyatas (42.8°N, 59.4°E) reports the highest frequency of dust storms in southwest Asia, 108 per year [*Middleton*, 1986b].

[58] There is also strong dust activity in the extreme southeast end of the Turan Plain, nestled against the mountains of Tajikistan (the Gissarskij Hrebet) and Afghanistan (the Hindu Kush) (Figures 4 and 5a, 37°N, 66°–67°E). The sources are mainly located in a valley that is the source of the Amu Darya (the ancient Oxus) River, which flows north between the Karakum desert and Kyzylkum desert and empties on the southern end of the Aral Sea. Because of the persistence of dust activity in this intermountain valley a large desert aerosol field study (the Joint Russian-American Desert Dust

Experiment) was held there in 1989 [*Golitsyn and Gillette*, 1993]. Vertical profiles made during the experiment showed that dust was well mixed to altitudes of 3–4 km, which would make the dust readily detectable by TOMS.

[59] The Caspian and Aral Seas are frequently cited as classic examples of major environmental disaster areas [*Stone*, 1999]. In the case of the Aral Sea much of the problem is associated with the damming after World War II of the Amu Darya, once the principal source of water, principally for irrigation. By the 1990s the river discharge into the Aral Sea was so reduced that flow ceased for periods of 1–3 months in most years (EB). Most of the lakes and bogs in the Amu Darya delta dried up, and its wetlands shrank to only a small percentage of their former size. Now the annual rate of evaporation of the Aral Sea far exceeds the rate of precipitation and the area has been dramatically reduced, exposing large areas of sediments on the eastern and southern shore [*Stone*, 1999]. The dried-out delta and exposed lake bottom are the most likely the sources of the dust detected by TOMS on the southern end of the Aral Sea.

[60] The Caspian Sea has also undergone large changes in water levels during historical times due to climate changes and human interventions (EB). In particular, in 1980, Soviet hydrologists reduced the outflow into the Garabogazköl by constructing sand barricades between the Caspian and the lagoon. Changes in water level lead to cycles of sediment deposition during high water stands and exposure and desiccation during low stands. The exposure of coastal and saline deposits coupled with the hot and arid climate of the eastern shore caused severe ecological problems from sulfate dust plumes being transported hundreds of kilometers [*Levine*, 1988] and is indicated by the dust sources seen in TOMS on the east shore. The dam across Garabogazköl was completely removed in 1992 after the independence of Turkmenistan.

4.3.2. Iran and Pakistan Basins

[61] A cluster of intermountain sources is located between the southern end of the Caspian Sea and the coast of the Arabian Sea in Iran and Pakistan (Figure 4). In TOMS, dust activity starts in April–May, becomes strong in June–July, and is greatly weakened by September (Figure 2), a cycle consistent with the seasonality of dust storm reports [*Middleton*, 1986b]. A major source area is located immediately to the south of the Caspian Sea in a large intermountain basin south of the Resht-eh-ye Kuhha-ye Alborz Mountains; the source extends from Tehran (35.6°N, 51.3°E) eastward to ~60°E (Figures 4 and 5a). Within the basin is the Dasht-e Kavir desert (48,000 km^2), which appears to consist largely of salt flats ("kavir," playa [*Gill*, 1996]). TOMS shows a particularly intense source centered over the western part of the basin (in the region close to Tehran) where there are many large drainage channels and a number of ephemeral lakes and marshes, including a large intermittent salt lake, Daryacheh-ye Mamak (1807 km^2).

[62] Another prominent cluster of sources lies in a basin centered at ~31°N, 61.5°E, straddling the border between Iran and Afghanistan (Figure 5a). The basin receives much runoff from the Seistan Mountains to the west in Iran and the eastern mountains in Afghanistan. The basin is characterized by widespread ephemeral lakes and swamps; in the northern part, there are many salt/dry lakes. SeaWiFS often shows huge dust plumes emerging from three of the largest, Hamun-e Saberi (31.5°N, 61.3°E), Hamun-e Puzak (31.5°N, 61.7°E), and Daryacheh-ye-Hamun (331.7°N, 61.1°E) and from the Gowd-e Zereh depression a little farther to the south (29.8°N, 61.8°E). Zabol, a city located in the midst of these salt/dry lakes, reports 81 dust storms per year [*Middleton*, 1986b]. In some years, dust activity is also seen in an intermountain basin to the south in Baluchistan, Pakistan; within this basin, there is a large dry lake (the Hamun-i-Mashkel, 1950 km^2; 28.2°N, 63.0°E), which is another prominent source of dust plumes in SeaWiFS.

[63] TOMS also shows considerable dust activity along the coast of the Persian Gulf and the Arabian Sea of Iran and Pakistan, on the southern flanks of the mountain chain that parallels the coast (Figures 2, September plot, 4, and 5a). There is one particularly active source in a small intermountain valley centered at 27.5°N, 59°E. At the center of this valley is a large salt/dry lake (Hamun-e Jaz Murian, 1087 km^2). Although many of the dust storms in these intermountain regions are quite intense, they are relatively small compared to those in other regions discussed thus far. Also, the plumes show a well-defined geometry. It has been suggested that these may be caused by intense low-level jets generated by the interaction of meteorology with the complex terrain [*Liu et al*., 2000]. The fact that so many of these sources in this region can be associated with salt/dry lakes suggests that the lakes themselves are important sources of dust. Many of the sources in the Iran-Afghanistan-Pakistan region contribute to the very high dust concentrations observed over the northern Arabian Sea [*Tindale and Pease*, 1999].

4.3.3. Indian Subcontinent

[64] Dust activity starts in March–April in northwest India in Rajasthan; activity peaks in May–June by which time all of northern India shows very high TOMS FOO values (Figures 2 and 5a) and AAI distributions (Figure 5f). By July, when the southwest monsoon has become well established, dust activity is largely confined once again to northwest India. The TOMS FOO distribution shows a sharply defined pattern across northern India. The mountain regions to the north, the Himalayas and the Hindu Kush, impart a strong topographical control on the dust sources and subsequent transport. The TOMS seasonality is consistent with the seasonal frequency of dust storm and dust haze reports from this region [*Ackerman and Cox*, 1989; *Middleton*, 1986b, 1989]. This region receives large amounts of runoff from

the mountains; these waters feed the Indus and Ganges river systems, producing over time extremely deep sediment deposits; loess deposits derived from large-scale Pleistocene glaciofluvial outwash [*Tripathi and Rajmani*, 1999] also serve as present-day dust sources [*Middleton*, 1986b]. In addition, large areas of Pakistan and the western region of north India are quite arid, and there are extensive desert regions, e.g., the Thar (Great Indian) Desert in Rajasthan, which contains a large saline lake and a long history of wind erosion [*Thomas et al*. 1999]. *Tripathi and Rajmani* [1999] suggest that this was a much more intense source of dust in the recent past, suggesting aeolian processes over a long period of time had selectively transported silt away, leaving behind the desert sands.

[65] Unfortunately, it is not possible to unambiguously attribute the high TOMS AAI over much of northern India solely to dust. The population density in this region is one of the highest in the world. Also much of India's heavy industry and mining is located here. Because of the lack of pollution controls, there are very large emissions of poorly combusted fuels of all types, including cooking and heating fires of wood and dung and emissions from millions of two-cycle and diesel engines. As a result, this region has the worst visibility conditions in the world [*Husar et al*., 2000]. Nonetheless, meteorological observations [*Middleton*, 1986b, 1989] show considerable dust activity across the entire region identified by TOMS.

[66] TOMS shows the highest FOO and AAI values over northwest India and Pakistan, covering an area extending from the coast of the Arabian Sea to the northern reaches of Pakistan, Punjab, and Rajasthan. This distribution extends over the Indus River basin and its tributaries to the north and the Thar (Great Indian) Desert (212,000 km^2) to the east. The maximum dust storm frequency is at Ganganagar (29.4°N, 71.7°E), located where the tributary system converges on the Indus River [*Middleton*, 1986b]. Dust storms occur to the east over the Ganges Plain, although the frequency decreases (at Delhi, 8 per year [*Middleton*, 1986b]) in agreement with the TOMS distributions. Large dust storms in northwest India are usually related to the easterly movement of a low-pressure zone or trough either at the surface or in the upper westerly wind regime [*Middleton*, 1986b, 1989]. This results in a steep pressure gradient and high winds, which can last for several days and produce dust storms over a wide area of northwest India and Pakistan. The dust is generally transported by pressure gradient winds to the east and northeast, down the Gangetic Plain as far as Bihar.

4.4. Asia

4.4.1. Introduction

[67] Studies show that every spring, large quantities of dust are generated in China by fronts that emerge from Siberia [*Goudie and Middleton*, 1992; *Middleton*, 1989, 1991; *Littmann*, 1991; *Prospero et al*., 1989; *Pye*, 1989]. Dust is carried out of China eastward, across the coastal waters and Korea to Japan [*Mukai et al*., 1990], where the dust is such a persistent phenomenon that it is given the name "kosa." Asian dust is routinely observed in relatively high concentrations at stations in the central North Pacific [*Arimoto et al*., 1996; *Prospero et al*., 1989; *Uematsu*, 1998; *Gao et al*., 2001], and it has been occasionally detected over North America. An Asian dust event in April 1998 yielded dust concentrations over the west coast states in the range 20–50 $\mu g\ m^{-3}$ with local peaks $>100\ \mu g\ m^{-3}$ [*Husar et al*., 2001]. Unfortunately, the interpretation of the TOMS product over Asia is complicated by frequent cloud cover and the presence of large amounts of pollutants, especially emissions from the burning of coal for heating and industrial purposes. In Figure 5g the high TOMS AAI values in east and southeast China in March, the peak of the dusty season, are attributed largely to pollution. The visual range in this region is known to be extremely poor at this time of year because of smoke [*Husar et al*., 2000]. Consequently, it is difficult to objectively identify dust sources separate from pollution sources in all cases. Nonetheless, in Figures 4, 5a, and 5g we can unambiguously identify a number of sources in western China: the Tarim Pendi and some adjacent basins.

4.4.2. Tarim Pendi and the Takla Makan Desert

[68] A large area in western China in Sinkiang (Xinjiang) Province shows high TOMS AAI values during much of the year. This is the Tarim Pendi basin (580,000 km^2), bounded by the Himalayan Plateau to the south, the mountains of the Hindu Kush to the west, and the Tien Shan to the north. The basin is huge, extending from ~75°E to 90°E between the latitudes 36°– 40°N. Persistent dust activity starts in February–March, reaches a maximum in April–May, and ends August–September (Figure 2). The geometry of the FOO distribution in Figures 5a and 5g closely matches the shape of the basin. The Tarim Basin receives very little rainfall, 50–100 mm a year along the periphery of the basin and ~10 mm in the central regions (EB). A large part of the basin is occupied by the Takla Makan desert, one of the largest in the world (272,000 km^2). Despite the low rainfall, the basin receives considerable runoff from the surrounding mountains. There are prominent features all along the edges of the basin, especially the northern side, which shows extensive river and stream channels and large areas of ephemeral lakes and marshes. Large alluvial fans slope toward the basin; these stand out prominently in satellite imagery [*Strain and Engle*, 1996]. The basin floor is covered with a several hundred meters thick layer of alluvial deposits.

[69] The easternmost extension of the TOMS AI distribution is located precisely over Lop Nor ("nor," salt lake) centered at ~90°E, 40°N. As recently as the 1950s, Lop Nor was a large (2000 km^2) saline lake (EB). Water diversion projects on the Tarim River, which drains the

Tarim Basin, reduced the inflow to such a degree that the lake is now an intermittent salt lake (324 km^2), largely salt-encrusted and subject to severe wind erosion. Meteorological observations [*Goudie and Middleton*, 1992] show that large-scale dust storms are associated with eastward moving fronts. Katabatic winds could also be important, especially in the Tarim Basin. Hotien (Khotan) on the southern edge of the Takla Makan experiences 33 dust storm days per year [*Goudie and Middleton*, 1992]; 67% of the dust events occur in March to June, a seasonality that is consistent with the TOMS record. There are many more days when dust storms do not occur at the meteorological station but when dense dust haze is reported. *Chen et al*. [1999] measured the chemical and physical characteristics of dust across a network of monitoring sites in the Takla Makan; monthly average <20-μm particulate concentrations ranged from 60 to 1250 $\mu g\ m^{-3}$.

[70] Three other intermountain sources can be seen in western China. Although these are relatively small, they demonstrate the sensitivity of dust sources to environmental conditions and the consistency among the sources. Immediately to the southeast of Lop Nor is an active region that appears as an appendage to the Tarim Basin distribution, the Qaidam Pendi (Tsaidam Basin; 37°N, 94°E), average elevation 2400–3000 m. Although the slopes of the enclosing mountains have grasslands, the interior portions are true desert interspersed with extensive playas, saline swamps, and hard salt deposits, including China's largest surface rock salt bed (1600 km^2) (EB). Total precipitation is <100 mm annually.

[71] Two moderately active sources are located north of the Tarim Basin. One, the Junggar (Dzungarian) Pendi, is centered at 45°N, 87°E (Figure 5a). This large basin (118,000 km^2) is formed by the Tien Shan Mountains to the south and the mountains of Kasakstan to the west and Russia and Mongolia to the north. The basin is quite arid (150–300 mm annually) (EB). There is drainage from the surrounding mountains, but little water reaches the central regions. Large saline lakes are found in the western regions, and the central and eastern end are covered with active sand dune systems. The second source is centered at (46°N, 75°E) in the western end of the Balqash-Alaköl Basin. The center of dust activity lies over the western end of the basin, where a large lake, Kazak Balqash (Ozero Balhas), is found. This lake has undergone great changes in recent times because of water diversion projects coupled with climate variability, and there are large areas of exposed sediments [*Bond et al*., 1992].

4.4.3. Other Asian Sources

[72] Studies of China dust transport often identify the Gobi desert, located east of the Tarim Basin on the Mongolian Plateau, as a major source of dust. Meteorological reports of dust storms show maximum activity (excluding the Tarim Basin) west of Beijing, including the Gobi, and south of Beijing [*Goudie*, 1983; *Dong et al*., 2000]. The huge trans-Pacific dust storm in April 1998, mentioned earlier, originated largely in the Gobi [*Husar et al*., 2001]. Similarly, in early April 2001, there was an extremely intense dust storm in this region that produced dust clouds that could be traced across North America into the North Atlantic. In contrast to the almost constant dust activity in the Tarim Basin the Gobi does not show persistent dust activity in TOMS FOO distributions. This is due in part to the fact that Gobi dust storms usually occur in response to strong winter storms that emerge from Siberia [*Middleton*, 1989, 1991; *Littmann*, 1991]. Clouds hamper detection with TOMS and reduce the FOO statistics. The Gobi is a stony desert, and we would not normally expect it to be a particularly strong source of dust [*Dong et al*., 2000] in comparison to the other sources described herein. Nonetheless, the Gobi is clearly a major source: *Xuan et al*. [2000] suggest that a zone in the central Gobi is subordinate only to the Takla Makan in terms of emission intensity of Chinese dust sources. This example serves to emphasize a point made earlier, that the TOMS sources discussed in this work represent a dominant class of sources but they are not the only important global dust sources. Nonetheless, we would expect on the basis of our study that dust sources in the Gobi desert have characteristics similar to those identified in TOMS elsewhere. Indeed, SeaWiFS images of dust storms in the Gobi often show that large dust clouds are comprised of many well-defined plumes that emerge from "point" sources. These might have characteristics that differ from the Gobi at large. They could be topographical lows similar to those of the TOMS dust sources, or they could be areas of the Gobi where the stony cover has been removed through human activities and agricultural development [*Dong et al*., 2000].

[73] There is evidence that wind erosion has increased in China over the past several decades, and it is argued [*Dong et al*., 2000] that humans are playing a role. Dong et al. studied wind erosion in arid and semiarid China, and they identify the main dust storm and soil erosion centers. Three of these are mapped by TOMS (Figure 5a): the Tarim Pendi and the Junggar and Qaidam Basins. In addition, they cite three other regions, all north of the Yellow River: the Alashan Gobi (including Badain Jaran desert, Tengger desert, Ulan Buh desert, and Hexi corridor), the northern Inner Mongolian Plateau, and the Horqin Steppe on the Ordos plateau. Dong et al. point out that many of the erosion centers are located on the Gobi desert and that "hardly any erosion occurs on the original deflation plane except when disturbed." They go on to argue that much of the erosion in these regions is due to rapid population growth in these regions, land reclamation, and agricultural development. However, at this time, it is not possible to quantify the impact of human-induced erosion on a larger scale.

[74] Finally, there are indications of dust activity over the Loess Plateau which lies north of the Qin Ling

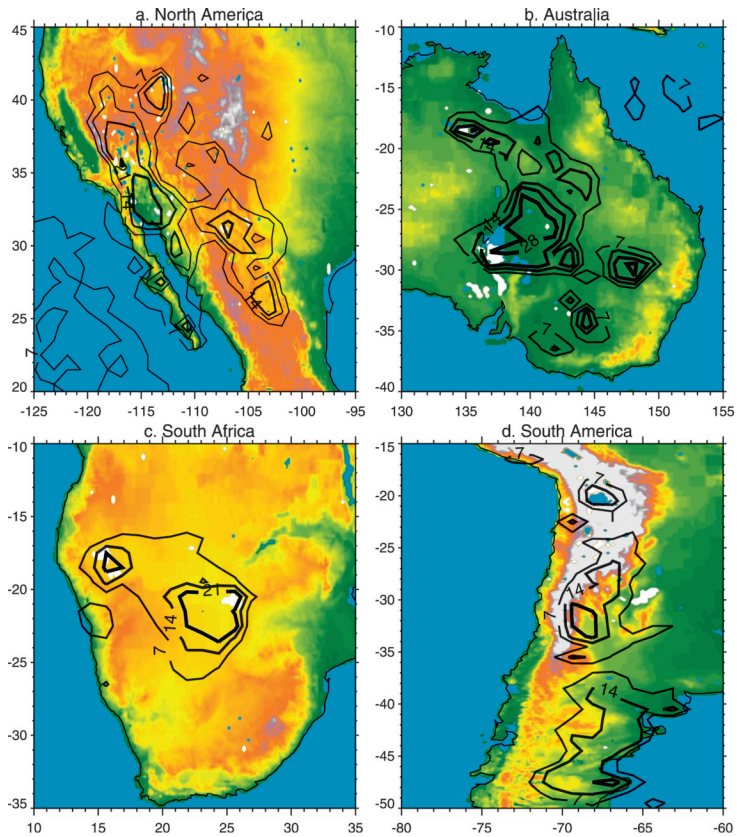

Figure 7. (a) North American dust sources. TOMS AAI frequency of occurrence distributions (days per month when the AAI equals or exceeds 0.7) are plotted as isolines on a topographic map. (b) Australian dust sources. TOMS AAI frequency of occurrence distributions (days per month when the AAI equals or exceeds 0.7) are plotted. (c) Southern African dust sources. TOMS AAI frequency of occurrence distributions (days per month when the AAI equals or exceeds 0.7) are plotted. (d) South American dust sources. TOMS AAI frequency of occurrence distributions (days per month when the AAI equals or exceeds 0.7) are plotted.

Mountains and the Wei River [*Zhang et al.*, 1997]. The Loess Plateau is a huge area (30,000 km^2) covered with loess, a wind-deposited soil [*Pye*, 1987], whose depths range from typically 30–60 m to as much as 200 m [*Pye*, 1987]. The Loess Plateau has long been suggested as a major dust source. These soils are now susceptible to enhanced deflation because of the intense agricultural activity in this region [*Dong et al.*, 2000].

5. OTHER DUST SOURCES

5.1. Introduction

[75] TOMS shows only modest amounts of dust activity outside the global dust belt (Figure 4). In North America, sources are visible in the western United States and northern Mexico. In the Southern Hemisphere, TOMS detects only a few relatively weak sources. Although small, they show persistent dust activity. In Australia, there is a large area in the Lake Eyre basin. In southern Africa, there is a source in Botswana in the region of the Makgadikgadi Pans; a second source is in Ovamboland in the region of the Etosha Pan. Finally, in South America, there are sources in the Altiplano, Bolivia, and in Argentina. Although all these sources are weak compared to the dust belt sources, we find that the environmental characteristics are similar.

5.2. North America

5.2.1. Western United States and Mexico

[76] The largest sources are located in the Basin and Range Province, a region roughly defined by the Sierra Nevada and Cascade ranges on the west, the Rocky Mountains on the east, the Columbia Plateau on the north, and the Mojave Desert and Colorado Plateau on the southwest [*Grayson*, 1993]. Additional sources are found farther to the south in the Basin and Range portion of northwestern Mexico (Figure 7a).

[77] A prominent area of activity is located immediately to the west and southwest of Great Salt Lake, Utah (41.3°N, 112.7W), which appears as the blue area on the NE side of the TOMS distribution in Figure 7a. Activity typically begins in April–May, reaches a peak in June–July, and ends in August–September. The active area extends over the Great Salt Lake Desert and the Bonneville Salt Flats; it terminates at the mountains to the west. The source is in a region once occupied by prehis-

toric Lake Bonneville, which in the late Pleistocene had an area of 52,000 km^2 (i.e., about as large as Lake Michigan); it covered much of present-day western Utah and extended into Nevada and Idaho [*Grayson*, 1993]. The Great Salt Lake is the remnant of the prehistoric lake, and Bonneville Salt Flats are the deposits left after evaporation. Today, this region is largely arid because of the blocking action of the Sierra Nevada, which strips moisture from the Pacific westerlies. Most precipitation (<120 mm annually) comes in the winter with air masses from the North Pacific and continental polar air [*Grayson*, 1993]; the seasonality is consistent with the summer maximum in dust activity.

[78] A second major source area is generally defined by the Salton Trough of southernmost California and northern Mexico. TOMS shows the most active sources to be largely defined by the coast of the Gulf of California to the south (at 114.5°N), the Peninsular Ranges to the west, and the Transverse Ranges to the north and northeast. This low-lying terrain includes the Sonoran Desert, Laguna Salada (a dry lake of 920 km^2), the Salton Sea, and a playa-rich region of the southwesternmost Mojave Desert. The dust activity extends eastward to ~111°E, to the Mogollon Rim at the SW edge of the Colorado Plateau. The dust season begins in April, reaches a maximum in May–June, and ends in August. As the season progresses, dust activity expands out of this region to the north-northwest. Immediately to the north lies an arid region that includes the Mojave Desert and the southwestern Basin and Range, where there is an extensive playa system including Owens Lake and Death Valley [*Grayson*, 1993]. Dust activity subsequently spreads north into the Great Basin reaching 40°–42°N in June–July. To the west the area of activity is largely defined by the Sierra Nevada. It extends to the east where in June it merges with the dusty area in the Great Salt Lake region. In general, there is less activity in the northern reaches of the Great Basin than in the areas farther to the south. A notable source in this region is seen around Carson Sink (40°N, 118°W), an intermittent dry lake which serves as the terminus of the Humboldt River [*Grayson*, 1993].

[79] In Mexico, there is a substantial but variably active source just south of the U.S.-Mexico border centered at 31°N, 107°W in the southern Mimbres Basin, where there is an extensive system of playas and aeolian, lacustrine, and alluvial sediments including Laguna Guzman and Bolson de los Muertos [*Hawley et al*., 2000] and the Medanos de Samalyuca [*Schmidt and Marston*, 1981]. At times the dust activity associated with this source extends north into the western end of the Llano Estacado in west Texas and southeastern New Mexico. There is a second center of activity farther to the southeast at 26°N, 103°W, also in the Basin and Range portion of Mexico.

5.2.2. Discussion: North American Sources

[80] The major TOMS dust sources in southwestern North America are located in topographical lows, many in intermountain regions. Dry lakes are common (Figure 7a). The Great Basin is largely arid; annual rainfall is 150–300 mm and supports little more than a sparse desert or semidesert vegetation (EB). This region received much more rain during the Pleistocene when lakes covered a remarkably large area (110,000 km^2 as compared to 10,000 km^2 today), a little over half of which was outside the Bonneville Basin [*Grayson*, 1993]. The sites of these former lakes now have deep accumulations of alluvial sediments, salt flats, and playas. *Reheis et al*. [1995] have shown that sediments discharged through alluvial fans or wadis emanating from proximate highlands are strong sources of dust along with materials deposited in recent pluvials [*Gill*, 1996; *Reheis and Kihl*, 1995; *Reheis*, 1997]. Thus the processes leading to the formation of strong dust sources in North America are fundamentally the same as those observed in North Africa.

[81] Dust emissions from this area have increased because of human activities, especially by water diversions for agriculture and other human uses both within the Great Basin and outside it, especially in California [*Bach et al*., 1996; *Grayson*, 1993]. An example is Owens Lake, which early in the twentieth century had an area of 280 km^2 [*Grayson*, 1993]. The lake disappeared after massive water diversions began in 1913 for use in the rapidly growing urban regions of southern California. Owens Lake is now a desolate salt flat which, ironically, is well known as the site of many studies of dust generation processes [*Cahill et al*., 1996; *Reheis*, 1997; *Gillette et al*., 1997, 2001].

[82] TOMS does not show much dust activity in the Great Plains, the site of the infamous "Dust Bowl" in the 1930s. Although dust emission in the boundary layer is still common in the region, only sporadic large-scale outbreaks lift dust to high altitudes [*Gill et al*., 2000]. Although most of the Great Plains experienced dust bowl conditions in the 1930s, the most intense activity was in the western third of Kansas, southeast Colorado, the Oklahoma Panhandle, the northern two thirds of the Texas Panhandle, and northeast New Mexico [*Goudie and Middleton*, 1992]. Dust emission in this region during the period of the TOMS data was at a historical minimum, thanks to short-term climatic variations and improved soil conservation practices [*Ervin and Lee*, 1994].

5.3. Australia

5.3.1. Lake Eyre and the Great Artesian Basin

[83] There is persistent dust activity in the Great Artesian Basin, which feeds Lake Eyre (Figures 4 and 7b), the largest playa in Australia. Activity starts late in the year, usually September–October, reaches a maximum in December–February, (i.e., the austral summer), and is

usually over by May. The TOMS seasonal cycle matches that measured in a network of dust sampling stations in southeastern Australia [*McTainsh and Lynch*, 1996]. During the period of maximum activity, the FOO distribution extends from Lake Eyre (27°S, 137°E) to the northeast over the Warburton Creek drainage region, to 24°–25°S, an area around the Diamantina River known as Channel Country. The southern limit of this active area lies on the northern flanks of the North Flinders Range. Maximum activity is centered on the northeast side of present-day Lake Eyre, in the heart of pluvial Lake Dieri ("ancestral Lake Eyre"), which was deflated of much of its sediments in the late Pleistocene [*Dulhunty*, 1982]. It is noteworthy that the Simpson Desert lies to the northwest of the active dust region seen in TOMS, but it does not appear in the FOO distribution, although large dust events occasionally emanate from this region [*Shao and Leslie*, 1997].

[84] The shape of the TOMS FOO distribution conforms to the general location of the Great Artesian Basin, a region (1,140,000 km^2) covered with vast sedimentary deposits [*Bridges*, 1990]. Because of the very small gradients (0.02–0.05%), rivers tend to be ephemeral, following braided or anastomosing courses from which the name "Channel Country" derives [*Bridges*, 1990]; during dry phases these serve as rich sources of dust [*Nickling et al*., 1999]. Rainfall over the basin is very low (<125 mm annually) and intermittent, most coming in winter from depressions moving in the westerlies. The timing of the dry season is consistent with the summertime maximum in TOMS values. Rivers and streams reach Lake Eyre only during very wet years. As a result, Lake Eyre is a salt lake (9300 km^2) that is normally largely dry; it fills completely only an average of twice in a century. There are also a number of salt/dry lakes to the south of Lake Eyre (Figure 7b). During the late Pleistocene, >10,000 years ago, the rainfall of central Australia was heavier than now; rivers carried large quantities of sediment and salt to the interior drainage basin of Lake Dieri [*Dulhunty*, 1982]. Today the basin is largely in an erosional phase.

5.3.2. Other Australian Sources

[85] There is a small area of weak and variable dust activity located east of the Great Basin at 30°S, 148°E in northern New South Wales on the northern side of the Darling River drainage system. This is relatively flat country, crossed with many rivers and streams that receive runoff from the Great Dividing Range to the east and to the north. Another small source is seen at 34°S, 145°E, in a region that receives drainage from the Great Dividing Range in New South Wales.

[86] High TOMS AAI values are sometimes seen across northern Australia in the Carpentaria Basin. One source is located in the Barkly Tableland (18°S, 136°E), a playa system and the site of a paleo–saline lake [*Ringrose*, 1996]. Occasional activity is seen in Queensland, extending from the Gulf of Carpentaria, approximately where the Flinders and Norman Rivers enter, to the western flanks of the Great Dividing Range. The activity is neither as intense nor as prolonged as that over the Great Basin, and furthermore, the activity varies greatly from year to year. However, the interpretation of the TOMS data is complicated by biomass burning, which is often prominent in this region.

[87] The areal distribution of dust activity shown in TOMS is markedly different from that based on observations of dust and haze made at meteorological stations across Australia [*Middleton*, 1984; *Shao and Leslie*, 1997]. This difference further emphasizes that ground-based measures of dust activity do not necessarily reflect the sources of dust that are important for long-range transport.

[88] The lack of strong dust activity elsewhere in Australia is surprising given that the continent is largely arid. Two thirds of the continent receives <500 mm of precipitation annually, and one third receives <250 mm; about one third of the land is desert, and another third is steppe or semidesert. The low dust output may be explained to some extent by the fact that the continent has relatively low topographical relief; only 6% is above 600-m elevation (EB). This stands in sharp contrast to the active dust sources in the Northern Hemisphere, most of which were associated with strongly defined topographical relief. Also, the terrains in Australia's arid regions are old and highly weathered; fine particles have long since been blown away.

5.4. Southern Africa

5.4.1. Makgadikgadi Depression and Pans, Botswana

[89] A persistent source is located in Botswana in the region centered at 21°S, 26°E (Figures 4 and 7c). The activity is highly variable from year to year. The interpretation of the TOMS product is complicated by widespread biomass burning in central Africa in July–September [*Hao and Liu*, 1994] when smoke is occasionally carried across Botswana. Although dust activity can usually be seen all year long, activity begins to increase strongly in June–July, tends to maximize in August–October, and then goes to a minimum over the austral winter.

[90] Dust activity is centered over the western end of the Makgadikgadi (formerly Makarikari) Depression, a region of sandy alkaline clay pans located southwest of the Okavango Delta, in the lowest part of the Kalahari desert, where a variety of lacustrine, fluvial, and aeolian landforms are in close juxtaposition [*Cooke and Verstappen*, 1984], just as in many of the other dust source areas elsewhere on Earth. The Makgadikgadi pans are among the world's largest, covering 22,051 km^2. In normal weather the pans consist of a series of shallow pools, sandy alkaline clays, and islands of grass. In Figure 7c the white area on the eastern side of the TOMS FOO distribution shows the Ntwetwe and Sowa Pans, the largest salt flats (4480 and 1116 km^2, respectively) in the

depression. During normal rainy seasons the pans are flooded by the Boteti River from the west, which, in turn, is fed by the Okavango River (and tributaries) from the north. During the Pleistocene the depression was occupied by a great lake, the Palaeo-Makgadikgadi which encompassed the Okavango Delta and large areas of northern Botswana, covering 120,000 km^2 [*Cooke and Verstappen*, 1984; *Goudie*, 1996].

5.4.2. Etosha Pan, Namibia

[91] A second small but persistent source is centered at 16°E, 18°S over the Etosha Pan, an extremely flat salt pan (4800 km^2) in northern Namibia. A number of relatively large ephemeral lakes and swamps lie to the west of the pan. The Etosha Pan is located in the extreme northwest of the Kalahari basin. Although the topographical relief is today rather weak at one time it was the former inland delta of the Cunene River, which originates in Angola; during the Pleistocene the Etosha Pan basin was occupied by a large lake [*Goudie*, 1996]. At some time in the past, river capture diverted the waters over the edge of the Great Escarpment at Ruacana Falls in Angola and now takes the river to the sea. Today, there is still drainage from the relatively higher (and wetter) regions in Angola to the Etosha Pan region via a network of ephemeral rivers and streams (EB).

[92] The Etosha Pan region offers a case study of human impacts. A large number of indigenous people were moved to this region as a "native homeland" (Ovamboland). Space shuttle photographs [*Strain and Engle*, 1996] clearly show the effects of land clearing, agriculture, and land degradation. These effects appear as a large region of relatively high surface albedo that extends north from the pan to the Angola border that stands out clearly in the image as a sharp boundary against the low-albedo terrain in Angola.

5.4.3. Discussion: Southern Africa Sources

[93] The annual dust cycle in the Etosha Pan is identical to that Makgadikgadi. During some years, TOMS shows dust activity across the entire region extending from the Makgadikgadi pans to the Etosha Pan. This region lies at the northern extremes of the Kalahari Basin and the Kalahari desert, the largest continuous sand surface in the world (EB). There are extensive sand/dune areas northwest of Makgadikgadi, large deflation pans to the southwest, and farther to the southwest, extensive dune systems [*Bridges*, 1990]. The fields of long parallel dunes, many of which are no longer active, have been attributed to drier paleoclimates that prevailed in the region in the late Quaternary [*Bridges*, 1990]. Nonetheless, TOMS does not show any strong or persistent dust activity in the Kalahari, although some weak activity is seen in December–January in some years. It is also notable that there is a third drainage system internal to the Kalahari [*Bridges*, 1990], the Malopo-Nassab, which formerly joined the Orange River. There are extensive ephemeral drainage systems in this area but no pans, ephemeral lakes, or swamps. TOMS does not show any dust in this region.

5.5. South America

5.5.1. Introduction

[94] The interpretation of TOMS data is difficult for large areas of South America because of the widespread burning especially over the Amazon where burning normally peaks in August–September [*Hsu et al*., 1996]. Although the burning is largely confined to moist areas where we do not expect to see much dust, smoke can be advected over large distances. Nonetheless, TOMS shows three areas that appear to be persistent dust sources: one in the Altiplano in Bolivia and two in Argentina (Figure 7d).

5.5.2. Altiplano, Bolivia

[95] TOMS shows a weak but persistent dust source in South America at 20°S, 67°W in the Bolivian Altiplano (Figures 4and 7d). The FOO statistics are variable from year to year, and the seasonality is not well defined. The maximum activity occurs late in the year, typically in September–November; the minimum is usually in April–June. The Bolivian Altiplano is an elevated intermountain basin that extends over ~1000 km, from southern Peru, across Bolivia, and into Argentina and Chile. The floor of the basin is at an altitude of 3750–4000 m, and it is ~200 km wide. The lower deposits of the basin are mainly sedimentary in origin, but more recent accumulations are volcanic. The southern Altiplano is arid and consists largely of desert; rains come mostly in December-January thunderstorms. There are many salt flats (salars) including Salar de Uyani (10,580 km^2) and the Salar de Coipasa (2220 km^2), two of the largest in the world [*Bridges*, 1990]. The TOMS FOO distribution in Figure 7d is centered directly over the salars (shown in blue). Space shuttle photos show many dust plumes over this region [*Strain and Engle*, 1996]. Shuttle imaging radar shows streaks of aeolian sediments aligned along prevailing winds [*Greeley et al*., 1989]. Many dust plumes are sharply defined as are the sediment streaks and can be directly traced to the salars and adjacent alluvial fans [*Goudie and Wells*, 1995]. During the late Pleistocene this region was filled with a lake which covered much of the Altiplano. The sediments from the former lake most likely serve as the source of the present-day dust activity.

5.5.3. Patagonia and Western Argentina

[96] There are two source areas in Argentina that show a moderately well defined seasonality and geometry. The southernmost distribution, in Patagonia between 38° and 48°S, is defined on the west by the Andes and by the flanks of the Meseta de Somuncurá, a very large high plateau (heights to ~2000 m) that extends east from the Andes; the dusty area extends to the Atlantic coast. Within this large region a particularly active area lies in the province of Neuquén, on the flanks

of the Andes, and in western Río Negro; it covers the southern Pampas and northern Patagonia. The Pampas in the west is dry and largely barren, with great saline areas, brackish streams, and sandy deserts. Northern Patagonia is a semiarid scrub (virtually treeless) plateau that extends from the Andes to the Atlantic coast, covering nearly all the southern portion of mainland Argentina (EB). Farther to the south in Santa Cruz (46°–48°S) is another active area, also characterized by aridity. This entire region is under the influence of the South Pacific westerlies. Moisture is largely removed from the air masses as they pass over the Andes, creating an extensive rain shadow zone on the eastern side of the mountain chain; consequently, rainfall is low, 100–180 mm annually (EB). There is extensive drainage from the eastern flanks of the Andes, but because most of Argentina is flat or gently sloping from the Andes to the Atlantic, river drainage is poor. Summer floods are common and leave behind ephemeral swamplands that gradually dry out in winter (EB).

[97] The region shows evidence of a long and varied climatic history. Deep, wide valleys bordered by high cliffs cut the tablelands from west to east; the valleys are the beds of former rivers that flowed from the Andes to the Atlantic. It is a region of glacial, glaciofluvial, and volcanic sediments derived from the Andes, now being modified by aeolian and fluvial processes [*Ferrer et al*., 1999]. The flat topography between the Andes and the Atlantic is made up of soils (fine sand, clay, and silt) washed down toward the Atlantic by rivers or blown in dust storms from the west. Most of the arid region is subjected to strong winds that carry sand and dust. Today, in Patagonia, windblown dust creates a continuous haze that considerably reduces visibility (EB). *Ramsperger et al*. [1998a, 1998b] made dust deposition measurements for a several year period at four sites along the coast in this region. They measured high deposition rates of Andes weathering products (which could be from the Pampas loessal soils themselves). They associated dust events with westerly winds sweeping down from the Andes. Dust emission in Santa Cruz has been linked to anthropogenic activities (overgrazing) that reduced vegetation cover and activated wind erosion over large areas of the province [*Iglesias*, 1992].

[98] A second major dust source is located in western Argentina roughly in the area between 27° and 34°S, 67° and 70°W along the eastern flanks of the Andes. Activity centers on an intermountain area between the Andes on the west and the Sierra de San Luis, Sierra de Comechingones, and Sierra de Cordoba on the east. The most active area lies in the western part of this region; the geometry and the northeast-southwest orientation of the spot on the west is defined by the flanks of the Andes. This region consists largely of arid and semiarid sections of sub-Andean ranges, foothills, and piedmont (EB). The land is laced with many small intermittent rivers and streams that often terminate in saline marshes, sand flats, and saline lakes, some among the largest in South America. These include Salinas Grandes (5500 km^2) and Salinas de Ambargasta (3100 km^2), the white area in Figure 7d at the northern end of the TOMS distribution at 30.5°S, 65°W.

5.5.4. Discussion: Southern Hemisphere Sources

[99] TOMS shows that the Southern Hemisphere is devoid of major dust sources that impact on large areas. This observation is consistent with aerosol measurements made in southern oceans which show that dust concentrations are very low, especially in comparison to many Northern Hemisphere ocean regions [*Prospero*, 1981, 1996a; *Gao et al*., 2001; *Heintzenberg et al*., 2000]. Also, the concentration of dust-derived Al in southern ocean waters is much lower than in northern oceans [*Measures and Vink*, 2000] as is the concentration of aeolian materials in deep-sea sediments [*Rea*, 1994]. Nonetheless, there is evidence that there was considerably more dust activity in the Southern Hemisphere in the past. Antarctic ice cores show that dust concentrations were sporadically much higher, most recently during the Last Glacial Maximum (LGM), ~20,000 years ago, when dust concentrations were ~30 times greater than today [*De Angelis et al*., 1992; *Gaudichet et al*., 1992; *Mayewski et al*., 1996]. The increased dust is broadly attributed to transport from continental sources in Australia, South America, and Africa and from exposed shelf sediments during low sea stands [*Harrison et al*., 2001]. The very low dust concentrations in the Holocene portions of the cores are consistent with the present-day dearth of dust sources in TOMS in the Southern Hemisphere and the low dust concentrations measured in field campaigns. Although it is not possible to identify sources active during the LGM, it is conceivable that the sites identified in TOMS today were much more active during the LGM. In particular, Patagonia was twice as large as today and was most likely a very intense dust source [*Iriondo*, 2000]. Also, the ancestral Lake Eyre basin was undergoing extreme deflation activity [*Dulhunty*, 1982]. There have been efforts to identify source provinces on the basis of distinctive properties of dust from ice cores, for example, individual particle analysis [e.g., *Gaudichet et al*., 1992]. It might be helpful to make similar measurements on the dust particles emitted from the sources identified in TOMS.

6. DISCUSSION AND CONCLUSIONS

6.1. Characteristics of Source Terrains

[100] TOMS shows a clear association of dust sources with specific types of landforms and environments. Almost all major sources are located in arid regions and are centered over topographical lows or on lands adjacent to strong topographical highs. Although the source regions themselves are arid or hyperarid, fluvial action is evident everywhere by the presence of ephemeral rivers and streams, alluvial fans, playas, and saline lakes. Fur-

thermore, most sources had a relatively recent pluvial history. The association of dust sources with water features is paradoxical but nonetheless consistent with our understanding of the processes involved in the production of fine particles through weathering. Fluvial and chemical weathering processes are much more efficient in the production of small particles (i.e., particles less than ~10-μm diameter) than are aeolian processes (i.e., grinding and impaction) [*Pye*, 1989]. Also, through fluvial action, small particles are separated from the soil and rock matrix and carried to depositional basins or alluvial plains where, after drying, they are subject to deflation by wind. This suggests that an important consideration with regard to precipitation is not only the amounts received in the source area itself but also the amounts received on the surrounding highlands where rainfall could be much greater, for example, the Tell Atlas feeding waters to the sources in northern Tunisia and Algeria, runoff from the Tibesti and Ahaggar mountains in central North Africa, and runoff from the Himalayas and the Tien Shan into the Tarim Basin. Similar processes are at work in arid intermountain basins which appear as sources in TOMS (e.g., in Pakistan, Iran, and Turkmenistan, Basin and Range lowlands in the United States and Mexico, and the Altiplano in South America).

[101] The most important characteristic of most major dust sources is the presence of deep and extensive alluvial deposits. During pluvial phases these basins were flooded, and thick layers of sediment were deposited and are now exposed. Many of the most active TOMS sources were flooded during the Pleistocene. The prime example is the Lake Chad Basin, the largest source of long-range dust in North Africa and possibly the world. With regard to the association of dust source with playas, *Reheis et al*. [1995] note that the strongest dust sources appear to be in the alluvial fans that ring the basins in which the playas are found. Similarly, *Yaalon* [1987] concludes that the major generic dust source in the Sahara "is weathered debris detrained by fluvial transport and redeposited on alluvial fans, in wadis, and terminal basins."

[102] TOMS shows a remarkably consistent association of dust sources with playas, a relationship that can be readily seen in Figures 5 and 7. There is considerable evidence that playas can be an important source of dust [*Gill*, 1996; *Reheis and Kihl*, 1995; *Reheis*, 1997; *Blank et al*., 1999]. It is our impression, however, that from the standpoint of large-scale dust processes the playas themselves are not necessarily the dominant sources within individual regions. Playa surfaces are often hardened and compacted, and they are often cemented with evaporites (e.g., gypsum or halite crusts) which armor the surface [*Cahill et al*., 1996; *Gillette et al*., 2001]. Rather, the close association of playas with TOMS sources is a manifestation of the general type of environment that is conducive to dust production: that is, arid basins that have had a recent pluvial history and which today receive relatively small amounts of water either directly or from runoff. In this regard, playas could serve as a convenient marker for potential dust source environments in the present or as evidence of active dust environments in the past. The playa is the ultimate receptacle of almost all the fine-grained sediments eroded within a basin over a geological time period; thus they are storehouses of fine, dry, unconsolidated (and thus wind-erodible) sediments often in amounts far in excess of production rates in the present climate.

[103] Although we have not made an extensive study of precipitation in the TOMS source areas, it is clear that these regions are quite arid: the Great Basin in the United States receives 120 mm or less annually; the Great Artesian Basin in Australia (Lake Eyre Basin) receives <125 mm; the Tarim Basin receives 50–100 mm; and Patagonia receives 100–180 mm. The relationship between dust activity and rainfall is most clearly demonstrated by the distribution of dust sources in North Africa; the southern boundary of these sources closely matches the 200–250 mm isohyets. *Goudie* [1983], in his study of global dust sources (based on observations of dust raised at meteorological stations), noted that dust storm frequency peaks in areas where annual rainfall is between 100 and 200 mm. TOMS shows that the upper limit of large-scale sources is ~200–250 mm. The association of the dust source boundary with the 200–250 mm isohyets is also consistent with the occurrence of vegetation coverage as measured by satellite-derived vegetation indices [*Nicholson et al*., 1998], which suggests that higher rainfall amounts enable the growth of vegetation that stabilizes soils against deflation [*Marticorena et al*., 1997a].

[104] TOMS shows that sand dune systems are not generally good sources of dust. This is not to say that dust is not derived from sand deserts but, rather, that they are not rich sources of the relatively fine particles that can be carried by winds to high altitudes and over great distances. Measurements of dust particle size distributions made at distances of a few hundred kilometers or more from the source show that the mass median diameter rapidly shifts to sizes under 10 μm; over the oceans the mass median diameter is typically several micrometers [*Duce*, 1995]. The size of particles in sand dunes and sand seas is on the order of tens to several hundred micrometers [*Lancaster*, 1995]; particles of this size have a very high Stokes settling velocity in air and, consequently, they will not be carried far by winds.

[105] Although sand particles themselves cannot be transported great distances, they play an important role in the dust generation process. Because of the aerodynamic properties of smooth, fine-grained soil surfaces (such as those often found in playas), dust is not readily mobilized unless the soil surface is disrupted [*Gillette et al*., 1982; *Gillette*, 1999]. The bombardment of the surface by wind-driven sand particles is a highly effective mechanism for grinding and shattering large particles into smaller particles and for ejecting fine particles into

the atmosphere [*Gillette et al*., 1998; *Gillette*, 1999]. TOMS shows that many of the major dust sources are adjacent to major sand seas. Thus the juxtaposition of playas and fluvial deposits with sand sources may have the effect of enhancing the output of fine dust particles.

[106] Our findings validate on a global scale the observations made at ground level: that water is an essential part of the dust-forming process and that alluvial deposits are the most abundant sources of dust [see, e.g., *Middleton et al*., 1986; *Pye*, 1989; *Rognon et al*., 1989; *Reheis et al*., 1995]. Indeed, *Middleton et al*. [1986] list a number of specific sites that they identify as rich sources of dust on the basis of conventional field studies; all but one of these are located in the source regions identified by TOMS. Our work goes beyond that of Middleton et al. and similar studies in that with TOMS we define the geographical extent and temporal activity of the source regions and we identify many more sites on a global scale (Figure 4).

6.2. Desertification and Dust Mobilization

[107] In relating our observations of dust to regional terrain and climate characteristics we have assumed that we are observing the results of "natural" processes. Yet over the past several decades, there has been much discussion about the long-term effects of drought and land use on soils in arid regions. It has been suggested that the end effect would be the encroachment of desert conditions that would be difficult to reverse. The term "desertification" was coined to describe this process. This concern was first voiced shortly after the colonialist expansion took place in Africa [*Thomas and Middleton*, 1994; *Mortimore*, 1998]. There are many estimates of the rate of "advancement" of the desert boundary [*Middleton and Thomas*, 1992; *Thomas and Middleton*, 1994; *Mortimore*, 1998]. If such a process were indeed taking place, then we would expect to see an increase in the emission and transport of dust as a consequence of the expanded desert area.

[108] Beginning in the late 1960s, North Africa has suffered from varying degrees of drought. Rainfall decreased by 25–40% during the period 1968–1997 relative to 1931–1960; every year in the 1950s was relatively wet, and nearly every year since 1970 has been anomalously dry [*Nicholson et al*., 2000]. Drought has been linked with the increased mobilization of dust in this region. In Mauritania the frequency of dust storms increased sharply [*Middleton*, 1989; *Goudie and Middleton*, 1992]. *Mbourou et al*. [1997] studied visibility records at 53 meteorological stations in North Africa over the period 1957–1987; they find that in the Sahel, there has been a systematic decrease in visibility that is highly correlated with the decrease in rainfall. The dust increase has affected very large areas. *Prospero and Nees* [1986] show that the dust concentration in the trade winds at Barbados increased sharply; during the height of the drought in the early 1980s, summertime dust concentrations at Barbados were several times greater than in predrought periods in the middle 1960s. Furthermore, the year-to-year concentration of dust in Barbados is highly correlated with the previous year's rainfall deficit in the Sahel [*Prospero and Nees*, 1986; *Prospero*, 1996a]. Similarly, *Middleton* [1989] finds an inverse relationship between dust storm frequency and the prior year rainfall at Nouakchott, which is on the coast of Mauritania.

[109] Recent evidence suggests, however, that there has been no net increase in desert expanse in the past few decades [*Thomas and Middleton*, 1994]. The region of greatest concern is the Sahel, which since the late 1960s, has been subject to varying degrees of drought and increased human pressures [*Nicholson et al*., 2000]. Yet recent satellite studies of vegetation cover in this region do not show any substantial change in the past 20 years or so. *Nicholson et al*. [1998] used AVHRR to calculate the greenness index over the period 1980–1995, a period that saw great changes in rainfall amounts, including one period of extremely intense drought in the early 1980s. Although they did observe large changes over short time periods in response to changes in rainfall amounts, there was no longer-term trend and no indication of desert "encroachment." Longer-term effects were noted in some areas because of activities such as grazing and fuel gathering, but these effects tended to be relatively localized.

[110] The absence of any major large-scale change in vegetation raises questions about the source (or mechanism) that is responsible for the increased dust. There could be a general decrease in soil moisture and fluvial and phreatic (groundwater) discharge to playas. *Middleton* [1987] suggests that drought might lead to the reactivation of dunes and sand sheets that have been stabilized by vegetation during relatively wet years. Weathering processes and climate changes often lead to the development of substantial deposits of soil in interdune regions [*Lancaster*, 1995]; these soils could serve as a source of fine-grained dust during arid periods. *Moulin et al*. [1997] suggest that increased dust measured over the Mediterranean is not due to increased dust generation but rather to decreased rainfall over the Mediterranean and Europe; consequently, less dust is washed out of the dust-laden African air masses during transit. To the contrary, TOMS does show increased dustiness over the source regions in the early 1980s, as shown in Figure 3. Alternatively, the increased dust could be due to meteorological changes associated with the drought aside from the decreased rainfall, e.g., higher wind speeds, increased gustiness, and decreased rainout of dust over the source areas (because of the increased occurrence of "dry" convective storms). Obviously, the question of causation is far from being resolved.

6.3. Modeling Dust Transport and the Impact on Climate

[111] There has been a considerable effort to use models to characterize the generation and transport of

dust and its impact on climate. A number of climate models have incorporated dust as an aerosol radiative forcing agent [*Miller and Tegen*, 1998; *Tegen and Miller*, 1998; *Intergovernmental Panel on Climate Change* (*IPCC*), 2001]. Modeling climate impacts is difficult at several levels. At the microscopic level, models need information about particle size, refractive index, and whether minerals are mixed externally (i.e., as discrete particles) or as aggregates [*Arimoto*, 2001; *Marticorena et al*., 1997b; *Tegen et al*., 1996; *Schulz et al*., 1998; *Sokolik and Toon*, 1999; *Harrison et al*., 2001]. At ground level the models must be able to incorporate the many complex factors that affect dust mobilization, including soil physical properties and vegetation cover [*Gillette*, 1999].

[112] Some regional models have had success in predicting dust events and the subsequent transport of dust [e.g., *Marticorena et al*., 1997b; *Guelle et al*., 2000], but models have not had great success in developing a globally applicable soil dust mobilization scheme. As a result, models have had difficulties in simulating the temporal and spatial concentration of dust and of dust properties on a global scale, most notably in the southern hemisphere. In the recent IPCC assessment [*IPCC*, 2001], eight different dust models yielded widely divergent results. For example, they often show huge plumes (comparable to those emerging from the west coast of North Africa and extending over the Atlantic) emerging from Australia, whereas in fact, very little dust is transported out of the continent. (Even regional-scale models have difficulty in quantitatively replicating dust events in Australia [*Shao and Leslie*, 1997].) TOMS (corroborated by other satellites such as SeaWiFS and AVHRR) rarely detects dust plumes emerging from Australia or any other Southern Hemisphere source (Figure 1). Indeed, large-scale dust storms are so unusual in Australia that when they do occur, each is well documented. *Knight et al*. [1995] describe an unusually large dust storm that occurred in early December 1987. The storm originated over the Channel Country in the Great Artesian (Lake Eyre) Basin, the source that we have identified in TOMS. The dust cloud passed over Brisbane where it yielded a 24-hour dust concentration of 149 $\mu g\ m^{-3}$, and the cloud eventually passed over New Zealand. The authors could only find records for a total of eight occasions since the beginning of the twentieth century when Australian dust was observed in New Zealand. This is consistent with the low concentrations of mineral aerosol measured over the Indian Ocean and western South Pacific [*Prospero*, 1981; *Heintzenberg et al*., 2000; *Gao et al*., 2001]. In contrast, at Barbados, daily dust concentrations over 100 $\mu g\ m^{-3}$ are measured at least several times each summer, and monthly mean summertime dust concentrations are typically in the range of 20–30 $\mu g\ m^{-3}$ [*Prospero and Nees*, 1986; *Li et al*., 1996]. Thus evidence suggests that dust transport out of Australia is orders of magnitude less than that out of Africa.

[113] The difficulties the models have with dust is understandable given the complexity of the dust generation process. As pointed out by *Gillette* [1999], dust generation is a highly nonlinear process that is dependent on many factors, many of which are site specific, a point that is emphasized by satellites that often show large dust storms emanating from "point" sources. Thus, in order to model dust sources, many models require very detailed knowledge of soil, terrain, climate, and meteorology [*Callot et al*., 2000], information that is lacking for vast areas of the Earth.

[114] The identification of dust sources with topographical lows has simplified the dust modeling process and has lead to improved results. *Ginoux et al*. [2001] model global dust sources by using a topographical factor in the source function, wherein the source emissions are weighted by comparing the elevation of each 1° by 1° grid point with elevations in the surrounding hydrological basin. Comparisons with satellite products show that the model produces much improved results with regard to source activity and dust transport distributions. The agreement with field observations of dust aerosols at distant locations is for the most part excellent.

6.4. Dust Production and Human Impacts

[115] There has been considerable interest in the role of humans in "desertification." In the past, this interest was motivated by concern about the loss of productive land. However, if dust has an impact on climate, then the role of humans in the destabilization of soil surfaces takes on an added dimension. Most research on the impact of land use has been motivated by concerns about soil conservation and more recently by health considerations. Work has largely focused on agricultural lands or specific "problem" sites such as Owens Lake [*Gill*, 1996]. As a result, efforts to model the effects of land use on dust generation are hampered by the almost complete absence of relevant information at a global level.

[116] *Tegen and Fung* [1995] attempted to estimate the effect of land use on dust mobilization on a global scale and concluded that 20–50% of the global dust load was derived from "disturbed soil." This estimate is widely quoted, but it is almost certainly too high. Tegen and Fung arrived at this estimate in the following way. They compared the seasonal output of their original global dust model (without the "disturbed soil" factor) to the AVHRR aerosol optical depth distributions of dust from North Africa [*Husar et al*., 1997]. Their model shows a large plume emerging from the Sahara in all four seasons. In contrast, AVHRR [*Husar et al*., 1997] and TOMS (Figures 1 and 2) show a marked seasonal shift in the source distribution; in wintertime the plume emerges from the southwest coast of North Africa and the coast on the Gulf of Guinea with little coming out of the Sahara. Tegen and Fung found that they could force a similar seasonal progression in their model plume by employing a "disturbed soil" factor based on land use in the Sahel. They applied this factor to disturbed soils on a global scale and thereby arrived at their estimate of the human impact on dust mobilization.

[117] Our results suggest that human impacts are probably much smaller than those estimated by Tegen and Fung. The TOMS data show that the strongest, largest, and most persistent sources in North Africa are in regions that are essentially uninhabited (Figures 4 and 5a). In particular, the Bodele Depression in the Lake Chad Basin is a remarkably strong dust source; on a global scale it yielded the highest mean TOMS aerosol index and the largest areas of high FOO distributions (Figure 6). TOMS shows that during the winter months, dust from this area is transported to the southwest (Figure 2, January and November plots) over the Gulf of Guinea and the southwest coast of Africa. Dust from the Lake Chad Basin is largely responsible for the prominent plume over the tropical North Atlantic during the winter months [*Husar et al*., 1997; *Herman et al*., 1997]. There is a long record of field observations that attribute the Harmattan dust to the Lake Chad Basin in general and the Bodele Depression in particular [*Adetunji et al*., 1979; *McTainsh and Walker*, 1982; *Kalu*, 1979], which as shown above (section 4.1.9), is essentially uninhabited. Similarly, we show that in general, the most intense sources were clustered around the base of the Ahaggar and Tibesti Mountains. These are extremely arid and harsh environments with extremely low population densities. In a recent study, *Middleton and Goudie* [2001] independently come to the same conclusions regarding the major sources in North Africa.

[118] Also, we find that the major dust sources in North Africa were located on the dry side of the 200–250 mm isohyet. Agricultural and grazing activities can be supported in regions with rainfall <200–250 mm, but they must be confined to relatively localized areas around point sources of water. Consequently, land degradation is limited to relatively small areas. Most agricultural and grazing activity takes place south of the 200–250 mm isohyets, where land use impacts are greatest but where we see relatively weak dust sources. Satellite studies of biomass fires and seasonal surface albedo changes [*Pinty et al*., 2000] show that the greatest agricultural burning occurs well to the south of the 200–250 mm isohyets.

[119] Nonetheless, humans clearly have had a substantial impact on dust mobilization. As we have noted, dust sources are often associated with water features. Because dust sources are located in arid lands, agriculture and livestock will tend to concentrate around these water features and to maximize the use of available water. *Goudie and Wells* [1995] state that animals are clearly identified as playing a role in the formation and augmentation of deflation pans. The most clearly visible example in TOMS of human impacts is in the region of the Caspian and Aral Seas, the result of the massive diversion of water for agriculture. As noted above, cultivation on the loess lands in China is blamed for much of the intense dust activity in this region and in large areas of inner Mongolia, Mongolia, and northeast China [*Dong et al*., 2000]. Similarly, in the southwestern North America, human impacts are a result of water diversion and agriculture. Perhaps the best and oldest example of the effects of agriculture is the Tigris-Euphrates river basin, the fertile crescent, the birth place of agriculture in the western world; the combined effects of 10,000 years of agriculture and climate change have turned this region into a major dust source. Although efforts to assess the consequences of human activity on large-scale dust mobilization have not been successful as yet, it is an important issue, one that will have to be addressed in a systematic and quantitative way.

6.5. Dust Transport, Climate, and Paleoclimate

[120] The pattern of dust transport and deposition to the oceans in the present-day shows large spatial variations which are related to the distribution of arid source regions and the character of the large-scale wind systems [*Duce et al*., 1991; *Prospero*, 1996a, 1996b; *Gao et al*., 2001]. Consequently, dust has long been used as a proxy indicator of continental aridity both in the study of deep-sea sediments [*Rea*, 1994] and in ice cores from Arctic regions [*Yung et al*., 1996; *De Angelis et al*., 1992; *Gaudichet et al*., 1992; *Kohfeld and Harrison*, 2001]. Our study shows that there are many factors other than aridity that impact on the rate of production of dust and its subsequent long-range transport. In particular, we show that the most active sources are associated with present-day fluvial processes and that the source regions have deep reservoirs of Quaternary alluvium generally deposited during pluvials. Old arid terrains such as those found over a large region of Australia are not good sources; neither are sand seas. Thus the best geomorphic environments for dust emission are those that have a relatively recent history of aridity and strong topographical relief. These environmental requirements complicate the paleoclimatic interpretation of dust transport because it suggests that dust is not so much an indicator of aridity as it is of a recent or present-day transition to aridity. These points have been made before [*Prospero*, 1985; *Pye*, 1989], but on the basis of our study we show that these conclusions are globally applicable. Given the difficulties that models have in replicating present-day dust sources and transport distributions, the results of attempts to model paleoclimate dust processes [e.g., *Mahowald et al*., 1999, *Reader et al*, 1999; *Harrison et al*., 2001] must be viewed with caution. Similarly, projections of dust mobilization in the future as a result of climate change and direct human impacts are fraught with difficulty [*IPCC*, 2001]

6.6. Future Directions for Dust Source Studies

[121] TOMS has proven to be an extremely valuable tool in identifying dust sources. The TOMS data will enable field scientists to design programs that focus on specific source areas so as to characterize the environments of these rich dust sources. Clearly, the "dust belt" is the dominant source today (Figure 4). What factors converge to make it so? Within the dust belt, North

Africa stands out as the strongest and most persistently active dust source. Why is this so, and why is it that within this larger region, there are some sources that stand out? In particular, the dust activity in the Bodele Depression is remarkable because of its activity and its intercontinental impact. The historical record suggests that this region has been active for at least several hundred years. What makes this source so active, and how can this source maintain this level of activity for so long? Furthermore, if dust does affect climate in some way [*Nicholson*, 2000], what impact has African dust had on the climate of North Africa and the tropical North Atlantic?

[122] The TOMS AAI product is also important because it shows us that there are arid regions where there is little or no dust. These too warrant study. For example, why is it that we see so little dust emerging in the present day from Australia? It is the most arid continent in the world, and it has extensive desert areas. This same question can be asked of the other arid regions that seem to yield so little dust. Such information is necessary for the development of models that can accurately depict dust mobilization processes and their subsequent effects on climate and on global-scale biogeochemical processes that involve dust.

[123] **ACKNOWLEDGMENTS.** This work was supported by the National Aeronautics and Space Administration (grants NAG57674 and NAG54020) and the National Science Foundation (grant NIBA-ATM-9521761), with contributions by the NASA TOMS processing team.

Thomas Torgersen was the editor responsible for this paper. He thanks Andrew Goudie and one anonymous reviewer for technical reviews.

REFERENCES

Ackerman, S. A., Remote sensing aerosols using satellite infrared observations, *J. Geophys. Res.*, *102*, 17,069–17,079, 1997.

Ackerman, S. A., and S. K. Cox, Surface weather observations of atmospheric dust over the southeast summer monsoon region, *Meteorol. Atmos. Phys.*, *41*, 19–34, 1989.

Adetunji, J., J. McGregor, and C. K. Ong, Harmattan haze, *Weather*, *34*, 430–436, 1979.

Arimoto, R., Eolian dust and climate: Relationships to sources, tropospheric chemistry, transport and deposition, *Earth Sci.Rev.*, *54*, 29–42, 2001.

Arimoto, R., R. A. Duce, B. J. Ray, W. G. Ellis Jr., J. D. Cullen, and J. T. Merrill, Trace elements in the atmosphere over the North Atlantic, *J. Geophys. Res.*, *100*, 1199–1214, 1995.

Arimoto, R., R. A. Duce, D. L. Savoie, J. M. Prospero, R. Talbot, J. D. Cullen, U. Tomza, N. F. Lewis, and B. J. Ray, Relationships among aerosol constituents from Asia and the North Pacific during PEM-West A, *J. Geophys. Res.*, *101*, 2011–2024, 1996.

Bach, A. J., A. J. Brazel, and N. Lancaster, Temporal and spatial aspects of blowing dust in the Mojave and Colorado deserts of southern California, 1973–1994, *Phys. Geogr.*, *17*, 329–353, 1996.

Blank, R. R., J. A. Young, and F. L. Allen, Aeolian dust in a saline playa environment, Nevada, USA, *J. Arid Environ.*, *41*, 365–381, 1999.

Bond, A. R., P. P. Micklin, and M. J. Sagers, Lake Balkhash dwindling, becoming increasingly saline, *Post Soviet Geogr.*, *33*, 131–134, 1992.

Bridges, E. M., *World Geomorphology*, 260 pp., Cambridge Univ. Press, New York, 1990.

Briere, P. R., Playa, playa lake, sabkha: Proposed definitions for old terms, *J. Arid Environ.*, *45*, 1–7, 2000.

Cahill, T. A., T. E. Gill, J. S. Reid, E. A. Gearhart, and D. A. Gillette, Saltating particles, playa crusts and dust aerosols at Owens (dry) Lake, California, *Earth Surf. Processes Landforms*, *21*, 621–639, 1996.

Callot, Y., B. Marticorena, and G. Bergametti, Geomorphologic approach for modelling the surface features of arid environments in a model of dust emissions: Application to the Sahara desert, *Geodin. Acta*, *13*(5), 245–270, 2000.

Chen, W., D. W. Fryrear, and Z. Yang, Dust fall in the Takla Makan desert of China, *Phys. Geogr.*, *20*, 189–224, 1999.

Chiapello, I., J. M. Prospero, J. R. Herman, and N. C. Hsu, Detection of mineral dust over the North Atlantic Ocean and Africa with the Nimbus 7 TOMS, *J. Geophys. Res.*, *104*, 9277–9292, 1999.

Chorowicz, J., and J. Fabre, Organization of drainage networks from space imagery in the Tanezrouft Plateau (western Sahara): Implications for recent intracratonic deformations, *Geomorphology*, *21*, 139–151, 1997.

Coe, M. T., and J. A. Foley, Human and natural impacts on the water resources of the Lake Chad basin, *J. Geophys. Res.*, *106*, 3349–3356, 2001.

Cooke, H. J., and T. Verstappen, The landforms of the western Makgadikgadi basin in northern Botswana, with a consideration of the chronology of the evolution of Lake Paleo-Makgadikgadi, *Z. Geomorph.*, *28*, 1–19, 1984.

Cornet, C., Middle Pleistocene hydrographic network on the Daoura Hamada (western Sahara) and consequences of its recent evolution, *Rev. Geomorph. Dyn.*, *39*, 39–45, 1990.

De Angelis, M., N. J. Barkov, and V. N. Petrov, Sources of continental dust over Antarctica during the last glacial cycle, *J. Atmos. Chem.*, *14*, 233–244, 1992.

Dentener, F. J., G. R. Carmichael, Y. Zhang, J. Lelieveld, and P. J. Crutzen, Role of mineral aerosol as a reactive surface in the global troposphere, *J. Geophys. Res.*, *101*, 22,869–22,889, 1996.

Dickerson, R. R., S. Kondragunta, G. Stenchikov, K. L. Civerolo, B. G. Doddridge, and B. N. Holben, The impact of aerosols on solar ultraviolet radiation and photochemical smog, *Science*, *278*, 827–830, 1997.

Dong, Z., X. Wang, and, L. Liu, Wind erosion in semiarid China: An overview, *J. Soil Water Conserv.*, *55*, 439–444, 2000.

Duce, R. A., Sources, distributions, and fluxes of mineral aerosols and their relationship to climate, in *Dahlem Workshop on Aerosol Forcing of Climate*, edited by R. J. Charlson and J. Heintzenberg, pp. 43–72, John Wiley, New York, 1995.

Duce, R. A., et al., The atmospheric input of trace species to the world ocean, *Global Biogeochem. Cycles*, *5*, 193–259, 1991.

Dulhunty, J. A., Holocene sedimentary environments in Lake Eyre, south Australia, *J. Geol. Soc. Aust.*, *29*, 437–442, 1982.

El-Sayed, M. I., Tidal flat rocks and sediments along the eastern coast of the United Arab Emirates, *Carb. Evaporites, 14*, 106–120, 1999.

Encyclopaedia Britannica, Britannica CD 2000 Deluxe Edition 1994–2000, Chicago, Ill., 2000.

Ervin, R. T., and J. A. Lee, Impact of conservation practices on

airborne dust in the southern High Plains of Texas, *J. Soil Water Conserv.*, *49*, 430–437, 1994.

Eugster, H. P., and G. Maglione, Brines and evaporites of the Lake Chad basin, Africa, *Geochim. Cosmochim. Acta*, *43*, 973–981, 1979.

Evans, G., C. G. S. C. Kendall, and P. Skipwith, Origin of the coastal flats, the sabkha, of the Trucial Coast, Persian Gulf, *Nature*, *202*, 759–761, 1964.

Falkowski, P. G., R. T. Barber, and V. Smetacek, Biogeochemical controls and feedbacks on ocean primary production, *Science*, *281*, 200–206, 1998.

Ferrer, J. A., F. X. Pereyra, and D. Villegas, Landforms and soils in the Traful River Valley, Neuquen Province, *Rev. Asoc. Geol. Argent.*, *54*, 270–280, 1999.

Fung, I., S. Meyn, I. Tegen, S. C. Doney, J. John, and J. K. B. Bishop, Iron supply and demand in the upper ocean, *Global Biogeochem. Cycles*, *14*, 281–296, 2000.

Gao, Y., Y. J. Kaufman, D. Tanre, D. Kolber, and P. G. Falkowski, Seasonal distributions of aeolian iron fluxes to the global ocean, *Geophys. Res. Lett.*, *28*, 29–32, 2001.

Gaudichet, A., M. De Angelis, S. Joussaume, J. R. Petit, Y. W. Korotkevitch, and V. N. Petrov, Comments on the origin of dust in East Antarctica for present and ice age conditions, *J. Atmos. Chem.*, *14*, 129–142, 1992.

Gill, T. E., Eolian sediments generated by anthropogenic disturbances of playas: Human impacts on the geomorphic system and geomorphic impacts on the human system, *Geomorphology*, *17*, 207–228, 1996.

Gill, T. E., D. L. Westphal, G. Stephens, and R. E. Peterson, Integrated assessment of regional dust transport from west Texas and New Mexico, spring 1999, paper presented at 11th Joint Conference on Applications of Air Pollution Meteorology, Am. Meteorol. Soc., Long Beach, Calif., 2000.

Gillette, D. A., Production of dust that may be carried great distances, in *Desert Dust: Origin, Characteristics, and Effect on Man*, edited by T. L. Pewe, *Spec. Pap. Geol. Soc. Am.*, *86*, 11–26, 1981.

Gillette, D. A., A qualitative geophysical explanation for "hot spot" dust emitting source regions, *Contrib. Atmos. Phys.*, *72*, 67–77, 1999.

Gillette, D. A., J. Adams, D. Muhs, and R. Kihl, Threshold friction velocities and rupture moduli for crusted desert soils for the input of soil particles into the air, *J. Geophys. Res.*, *87*, 9003–9015, 1982.

Gillette, D. A., E. Hardebeck, and J. Parker, Large-scale variability of wind erosion mass flux rates at Owens Lake, 2, Role of roughness change, particle limitation, change of threshold friction velocity, and the Owen effect, *J. Geophys. Res.*, *102*, 25,989–25,998, 1997.

Gillette, D. A., B. Marticorena, and G. Bergametti, Change in the aerodynamic roughness height by saltating grains: Experimental assessment, test of theory, and operational parameterization, *J. Geophys. Res.*, *103*, 6203–6210, 1998.

Gillette, D. A., T .C. Niemeyer, and P. J. Helm, Supply-limited horizontal sand drift at an ephemerally crusted, unvegetated saline playa, *J. Geophys. Res.*, *106*, 18,085–18,098, 2001.

Ginoux, P., M. Chin, I. Tegen, J. M. Prospero, B. Holben, O. Dubovik, and S.-J. Lin. Sources and distributions of dust aerosols simulated with the GOCART model, *J. Geophys. Res.*, *106*, 20,255–20,274, 2001.

Golitsyn, G., and D. A. Gillette, Introduction: A joint Soviet-American experiment for the study of Asian desert dust and its impact on local meteorological conditions and climate, *Atmos. Environ., Part A*, *27*, 2467–2470, 1993.

Goudie, A. S., Dust storms in space and time, *Prog. Phys. Geogr.*, *7*, 502–530, 1983.

Goudie, A. S., Climate, past and present, in *The Physical Geography of Africa*, edited by W. M. Adams, A. S. Goudie, and A. R. Orme, pp. 44–59, Oxford Univ. Press, New York, 1996.

Goudie, A. S., and N. J. Middleton, The changing frequency of dust storms through time, *Clim. Change*, *20*, 197–225, 1992.

Goudie, A. S., and G. L. Wells, The nature, distribution, and formation of pans in arid areas, *Earth Sci. Rev.*, *38*, 1–69, 1995.

Grayson, D. K., *The Desert's Past: A Natural History of the Great Basin*, 356 pp., Smithsonian Inst. Press, Washington, D. C., 1993.

Greeley, R., P. Christensen, and R. Carrasco, Shuttle radar images of wind streaks in the Altiplano, Bolivia, *Geology*, *17*, 665–668, 1989.

Grunert, J., R. Baumhauer, and J. Volkel, Lacustrine sediments and Holocene climates in the southern Sahara: The example of paleolakes in the Grand Erg of Bilma (Zoo Baba and Dibella, eastern Niger), *J. Afr. Earth Sci.*, *12*, 133–146, 1991.

Guelle, W., Y. J. Balkanski, M. Schulz, B. Marticorena, G. Bergametti, C. Moulin, R. Arimoto, and K. D. Perry, Modeling the atmospheric distribution of mineral aerosol: Comparison with ground measurements and satellite observations for yearly and synoptic timescales over the North Atlantic, *J. Geophys. Res.*, *105*, 1997–2012, 2000.

Guerzoni, S., and R. Chester (Eds), *The Impact of Desert Dust Across the Mediterranean*, 389 pp., Kluwer Acad., Norwell, Mass., 1996.

Hao, W. M., and M-H. Liu, Spatial and temporal distribution of tropical biomass burning, *Global Biogeochem. Cycles*, *8*, 495–503, 1994.

Harrison, S. P., K. E. Kohfeld, C. Roelandt, and T. Claquin, The role of dust in climate changes today, at the Last Glacial Maximum and in the future, *Earth Sci. Rev.*, *54*, 43–80, 2001.

Hawley, J. W., B. J. Hibbs, J. F. Kennedy, B. J. Creel, M. D. Remmenga, M. Johnson, M. M. Lee, and P. Dinterman, Trans-international boundary aquifers in southwestern New Mexico, *Rep. X-996350-01-03*, N. M. Water Resour. Res. Inst., Las Cruces, 2000.

Haywood, J., and O. Boucher, Estimates of the direct and indirect radiative forcing due to tropospheric aerosols, *Rev. Geophys.*, *38*, 513–543, 2000.

Heintzenberg, J., D. C. Covert, and R. Van Dingenen, Size distribution and chemical composition of marine aerosols: A compilation and review, *Tellus*, *Ser. B, 52*, 1104–1122, 2000.

Herman, J. R., and E. A. Celarier, Earth surface reflectivity climatology at 340–380 nm from TOMS data, *J. Geophys. Res.*, *102*, 28,003–28,012, 1997.

Herman, J. R., P. K. Bhartia, O. Torres, C. Hsu, C. Seftor, and E. Celarier, Global distribution of UV-absorbing aerosols from Nimbus-7/TOMS data, *J. Geophys. Res.*, *102*, 16,911–16,922, 1997.

Herrmann, L., K. Stahr, and R. Jahn, The importance of source region identification and their properties for soil derived dust: The case of Harmattan dust sources for eastern West Africa, *Contrib. Atmos. Phys.*, *72*, 141–150, 1999.

Hildebrand's Travel Map, United Arab Emirates, Oman, scale 1:1,500,000, Karto+Grafik, Frankfurt, Germany, 1996.

Hsu, N. C., J. R. Herman, P. K. Bhartia, C. J. Seftor, O. Torres, A. M. Thompson, J. F. Gleason, T. F. Eck, and B. N. Holben, Detection of biomass burning smoke from TOMS measurements, *Geophys. Res. Lett.*, *23*, 745–748, 1996.

Hsu, N. C., J. R. Herman, O. Torres, B. N. Holben, D. Tanre, T. F. Eck, A. Smirnov, B. Chatenet, and F. Lavenu, Comparisons of the TOMS aerosol index with Sun-photometer aerosol optical thickness: Results and applications, *J. Geophys. Res.*, *104*, 6269–6280, 1999.

Husar, R. B., J. M. Prospero, and L. L. Stowe, Characterization of tropospheric aerosols over the oceans with the NOAA advanced very high resolution radiometer optical thickness operational product, *J. Geophys. Res.*, *102*, 16,889–16,909, 1997.

Husar, R. B., J. D. Husar, and L. Martin, Distribution of continental surface aerosol extinction based on visual range data, *Atmos. Environ.*, *34*, 5067–5078, 2000.

Husar, R. B., et al., Asian dust events of April 1998, *J. Geophys. Res.*, *106*, 18,317–18,330, 2001.

Iglesias, A. N., Wind erosion, desertification and productivity crisis in the livestock economy of Patagonia: The case of the province of Santa Cruz, *Estud. Geograf.*, *53*, 4470–4479, 1992.

Intergovernmental Panel on Climate Change (IPCC), *Climate Change 2001: The Scientific Basis, Contribution of Working Group I to the Third Assessment Report of the Intergovernmental Panel on Climate Change*, edited by J. T. Houghton et al., 881 pp., Cambridge Univ. Press, New York, 2001.

Iriondo, M., Patagonian dust in Antarctica, *Quat. Int.*, *68*, 83–86, 2000.

Kalu, A. E., The African dust plume: Its characteristics and propagation across West Africa in winter, in *Saharan Dust: Mobilization, Transport, and Deposition, SCOPE 14*, edited by C. Morales, pp. 95–118, John Wiley, New York, 1979.

Knight, A. W., G. H. McTainsh, and R. W. Simpson, Sediment loads in an Australian dust storm: Implications for present and past dust processes, *Catena*, *24*, 195–213, 1995.

Kohfeld, K. E., and S. P. Harrison, DIRTMAP: The geological record of dust, *Earth Sci. Rev.*, *54*, 81–114, 2001.

Lancaster, N., *Geomorphology of Desert Dunes*, 279 pp., Routledge, New York, 1995.

Lancaster, N., Desert environments, in *The Physical Geography of Africa*, edited by W. M. Adams, A. S. Goudie, and A. R. Orme, pp. 211–237, Oxford Univ. Press, New York, 1996.

Levin, Z., E. Ganor, and V. Gladstein, The effects of desert particles coated with sulfate on rain formation in the eastern Mediterranean, *J. Appl. Meteorol.*, *35*, 1511–1523, 1996.

Levine, R. M., Mineral Industry of U.S.S.R., *Miner. Yearbk.*, *3*, 789–790, 1988.

Lev-Yadun, S., A. Gopher, and S. Abbo, The cradle of agriculture, *Science*, *288*, 1602–1603, 2000.

Li, X., H. Maring, D. Savoie, K. Voss, and J. M. Prospero, Dominance of mineral dust in aerosol light scattering in the North Atlantic trade winds, *Nature*, *380*, 416–419, 1996.

Littmann, T., Dust storm frequency in Asia: Climatic control and variability, *Int. J. Climatol.*, *11*, 393–412, 1991.

Liu, M., D. L. Westphal, T. R. Holt, and Q. Xu, Numerical simulation of a low-level jet over the complex terrain in southern Iran, *Mon. Weather Rev.*, *128*, 1309–1327, 2000.

Macmillan, *Planet Earth McMillan World Atlas*, Macmillan, New York, 1997.

Maenhaut, W., I. Salma, J. Cafmeyer, H. J. Annegarn, and M. O. Andrae, Regional atmospheric aerosol composition and sources in the eastern Transvaal, South Africa, and impact of biomass burning, *J. Geophys. Res.*, *101*, 23,631–23,650, 1996.

Mahowald, N., K. Kohfeld, M. Hansson, Y. Balkanski, S. P. Harrison, I. C. Prentice, M. Schulz, and H. Rodhe, Dust sources and deposition during the Last Glacial Maximum and current climate: A comparison of model results with paleodata from ice cores and marine sediments, *J. Geophys. Res.*, *104*, 15,895–15,916, 1999.

Marticorena, B., G. Bergametti, D. Gillette, and J. Belknap, Factors controlling threshold friction velocity in semiarid and arid areas of the United States, *J. Geophys. Res.*, *102*, 23,277–23,288, 1997a.

Marticorena, B., G. Bergametti, B. Aumont, Y. Callot, C. N'Doumé, and M. Legrand, Modeling the atmospheric dust cycle, 2, Simulation of Saharan dust sources, *J. Geophys. Res.*, *102*, 4387–4404, 1997b.

Mayewski, P. A., et al., Climate change during the last glaciation in Antarctica, *Science, 272*, 1636–1638, 1996.

Mbourou, G. N., J. J. Bertrand, and S. E. Nicholson, The diurnal and seasonal cycles of wind-borne dust over Africa north of the equator, *J. Appl. Meteorol.*, *36*, 868–882, 1997.

McTainsh, G. H., and A. W. Lynch, Quantitative estimates of the effect of climate change on dust storm activity in Australia during the Last Glacial Maximum, *Geomorphology*, *17*, 263–271, 1996.

McTainsh, G. H., and J. R. Pitblado, Dust storms and related phenomena measured from meteorological records in Australia, *Earth Surf. Processes Landforms*, *12*, 415–424, 1987.

McTainsh, G. H., and P. H. Walker, Nature and distribution of Harmattan dust, *Z. Geomorph.*, *26*, 417–435, 1982.

Measures, C. I., and S. Vink, On the use of dissolved aluminum in surface waters to estimate dust deposition to the ocean, *Global Biogeochem. Cycles*, *14*, 317–328, 2000.

Michaels, A. F., D. Olson, J. L. Sarmineto, J. W. Ammerman, K. Fanning, R. Jahnke, A. H. Knap, F. Lipschultz, and J. M. Prospero, Inputs, losses and transformations of nitrogen and phosphorus in the pelagic North Atlantic Ocean, *Biogeochemistry*, *35*, 181–226, 1996.

Middleton, N. J., Dust storms in Australia: Frequency, distribution and seasonality, *Search*, *15*, 46–47, 1984.

Middleton, N. J., Dust storms in the Middle East, *J. Arid Environ.*, *10*, 83–96, 1986a.

Middleton, N. J., A geography of dust storms in south-west Asia, *J. Climatol.*, *6*, 183–196, 1986b.

Middleton, N. J., Desertification and wind erosion in the western Sahel: The example of Mauritania, *Sch. Geogr. Res. Pap.* 40, 26 pp., Oxford Univ., Oxford, UK, 1987.

Middleton, N. J., Climatic controls on the frequency, magnitude and distribution of dust storms: Examples from India/Pakistan, Mauritania and Mongolia, in *Paleoclimatology and Paleometeorology: Modern and Past Patterns of Global Atmospheric Transport*, edited by M. Leinen and M. Sarnthein, pp. 97–132, Kluwer Acad., Norwell, Mass., 1989.

Middleton, N. J., Dust storms in the Mongolian People's Republic, *J. Arid Environ.*, *20*, 287–297, 1991.

Middleton, N. J, and A. S. Goudie, Saharan dust: Sources and trajectories, *Trans. Inst. Br. Geogr.*, *26*, 165–181, 2001.

Middleton, N. J., and D. S. G. Thomas (Eds.), *World Atlas of Desertification*, 66 pp., Edward Arnold, London, 1992.

Middleton, N. J., A. S. Goudie, and G. L. Wells, The frequency and source areas of dust storms, in *Aeolian Geomorphology*, edited by W. G. Nickling, pp. 237–259, Allen and Unwin, New York, 1986.

Miller, R. L., and I. Tegen, Climate response to soil dust aerosols, *J. Clim.*, *11*, 3247–3267, 1998.

Mortimore, M., *Roots in the African Dust: Sustaining the Sub-Saharan Drylands*, 219 pp., Cambridge Univ. Press, New York, 1998.

Moulin, C., C. E. Lambert, F. Dulac, and U. Dayan, Control of atmospheric export of dust from North Africa by the North Atlantic Oscillation, *Nature*, *387*, 691–694, 1997.

Moulin, C., et al., Satellite climatology of African dust transport in the Mediterranean atmosphere, *J. Geophys. Res.*, *103*, 13,137–13,143, 1998.

Mukai, H., Y. Ambe, K. Shibata, T. Muku, K. Takeshita, T. Fukuma, J. Takahashi, and S. Mizota, Long-term variation of chemical composition of atmospheric aerosol of the Oki Islands in the Sea of Japan, *Atmos. Environ., Part A*, *24*, 1379–1390, 1990.

Nicholson, S., Land surface processes and Sahel climate, *Rev. Geophys*, *38*, 117–139, 2000.

Nicholson, S. E., C. J. Tucker, and M. B. Ba, Desertification,

drought and surface vegetation: An example from the West African Sahel, *Bull. Am. Meteorol. Soc.*, *79*, 815–829, 1998.

Nicholson, S. E., B. Some, and B. Kone, A note on recent rainfall conditions in West Africa, including the rainy season of the 1997 ENSO year, *J. Clim.*, *13*, 2628–2640, 2000.

Nickling, W. G., G. H. McTainsh, and J. F. Leys, Dust emissions from the Channel Country of western Queensland, Australia, *Z. Geomorphol. Supp.*, *116*, 1–17, 1999.

Pachur, H. J., Lake Ptolemy in western Nubia as an indicator of paleoclimate, *Petermanns Geogr. Mittel.*, *141*, 227–250, 1997.

Perry, K. D., T. A. Cahill, R. A. Eldred, D. D. Dutcher, and T. E. Gill, Long-range transport of North African dust to the eastern United States, *J. Geophys. Res.*, *102*, 11,225–11,238, 1997.

Pinty, B., M. M. Verstraete, and N. Gobron, Do man-made fires affect Earth's surface reflectance at continental scales?, *Eos Trans. AGU*, *81*, 381, 388–389, 2000.

Prospero, J. M., Aeolian transport to the World Ocean, in *The Sea*, vol. 7, *The Oceanic Lithosphere*, edited by C. Emiliani, pp. 801–974, Wiley Interscience, New York, 1981.

Prospero, J. M., Records of past climates in deep sea sediments, *Nature*, *315*, 279–280, 1985.

Prospero, J. M., The atmospheric transport of particles to the ocean, in *Particle Flux in the Ocean*, edited by V. Ittekkott, S. Honjo, and P. J. Depetris, *SCOPE Rep. 57*, pp. 19–52, John Wiley, New York, 1996a.

Prospero, J. M., Saharan dust transport over the North Atlantic Ocean and Mediterranean: An overview, in *The Impact of Desert Dust Across the Mediterranean*, edited by S. Guerzoni and R. Chester, pp. 133–151, Kluwer Acad., Norwell, Mass., 1996b.

Prospero, J. M., Long-term measurements of the transport of African mineral dust to the southeastern United States: Implications for regional air quality, *J. Geophys. Res.*, *104*, 15,917–15,927, 1999.

Prospero, J. M., and R. T. Nees, Impact of the North African drought and El Niño on mineral dust in the Barbados trade winds, *Nature*, *320*, 735–738, 1986.

Prospero, J. M., R. A. Glaccum, and R. T. Nees, Atmospheric transport of soil dust from Africa to South America, *Nature*, *289*, 570–572, 1981.

Prospero, J. M., M. Uematsu, and D. L. Savoie, Mineral aerosol transport to the Pacific Ocean, in *Chemical Oceanography*, vol. 10, edited by J. P. Riley, R. Chester and R. A. Duce, pp. 188–218, Academic, San Diego, Calif., 1989.

Pye, K., *Aeolian Dust and Dust Deposits*, 334 pp., Academic, San Diego, Calif., 1987.

Pye, K., Processes of fine particle formation, dust source regions, and climatic changes, in *Paleoclimatology and Paleometeorology: Modern and Past Patterns of Global Atmospheric Transport*, edited by M. Leinen and M. Sarnthein, pp. 3–30, Kluwer Acad., Norwell, Mass., 1989.

Quarmby, N. A., J. R. G. Townshend, A. C. Millington, K. White, and A. J. Reading, Monitoring sediment transport systems in a semiarid area using Thematic Mapper data, *Remote Sens. Environ.*, *28*, 305– 315, 1989.

Ramsperger, B., L. Herrmann, and K. Stahr, Dust characteristics and source-sink relations in eastern West Africa (SW-Niger and Benin) and South America (Argentinian Pampas), *Z. Pflanzenernahr. Bodenk.*, *161*, 357–363, 1998a.

Ramsperger, B., N. Peinemann, and K. Stahr, Deposition rates and characteristics of aeolian dust in the semi-arid and sub-humid regions of the Argentinian Pampa, *J. Arid Environ.*, *39*, 467– 476, 1998b.

Rand McNally, *The Great Geographical Atlas*, Skokie, Ill., 1991.

Rand McNally, *New Millennium World Atlas Deluxe* [CD-ROM], Skokie, Ill., 1998.

Rea, D. K., The paleoclimatic record provided by eolian deposition in the deep sea: The geologic history of wind, *Rev. Geophys.*, *32*, 159–195, 1994.

Reader, M. C., I. Fung, and N. McFarlane, The mineral dust aerosol cycle during the Last Glacial Maximum, *J. Geophys. Res.*, *104*, 9381–9398, 1999.

Rebillard, P., and J. L. Ballais, Surficial deposits of two Algerian playas as seen on SIR-A, Seasat and Landsat coregistered data (Chotts Merouan and Melrhir, Sahara), *Z. Geomorphol.*, *28*, 483– 498, 1984.

Reheis, M., Dust deposition downwind of Owens (dry) Lake, 1991–1994: Preliminary findings, *J. Geophys. Res.*, *102*, 25,999–26,008, 1997.

Reheis, M. C., and R. Kihl, Dust deposition in southern Nevada and California, 1984–1989: Relations to climate, source area, and source lithology, *J. Geophys. Res.*, *100*, 8893–8918, 1995.

Reheis, M. C., J. C. Goodmacher, J. W. Harden, L. D. McFadden, T. K. Rockwell, R. R. Shroba, J. M. Sowers, and E. M. Taylor, Quaternary soils and dust deposition in southern Nevada and California, *Geol. Soc. Am. Bull.*, *107*, 1003–1022, 1995.

Ringrose, S., The geomorphological context of calcrete deposition in the Dalmore Downs area, Northern Territory, Australia, *J. Arid Environ.*, *33*, 291–307, 1996.

Rognon, P., G. Coude-Gaussen, G. Bergametti, and L. Gomes, Relationships between the characteristics of soils, the wind energy and dust near the ground, in the western sandsea (N.W. Sahara), in *Paleoclimatology and Paleometeorology: Modern and Past Patterns of Global Atmospheric Transport*, edited by M. Leinen and M. Sarnthein, pp. 167–184, Kluwer Acad., Norwell, Mass., 1989.

Rosen, M. R., The importance of groundwater in playas: A review of playa classifications and the sedimentology and hydrology of playas, *Spec. Pap. Geol. Soc. Am.*, *289*, 1–18, 1994.

Satchell, J. E., M. D. Mountford, and W. M. Brown, A land classification of the United Arab Emirates, *J. Arid Environ.*, *4*, 275–285, 1981.

Satheesh, S. K., V. Ramanathan, X. Li-Jones, J. M. Lobert, I. A. Podgorny, J. M. Prospero, B. N. Holben, and N. G. Loeb, A model for the natural and anthropogenic aerosols over the tropical Indian Ocean derived from Indian Ocean Experiment data, *J. Geophys. Res.*, *104*, 27,421–27,440, 1999.

Savoie, D. L., J. M. Prospero, and R. T. Nees, Nitrate, non-sea-salt sulfate, and mineral aerosol over the northwestern Indian Ocean, *J. Geophys. Res.*, *92*, 933–942, 1987.

Schmidt, R. H., Jr., and R. A. Marston, Los Medanos de Samalayuca, Chihuahua, Mexico, *N. M. J. Sci*, *21*(2), 21–27, 1981.

Schroeder, J. H., Eolian dust in the coastal desert of Sudan: Aggregates cemented by evaporates, *J. Afr. Earth Sci.*, *3*, 371–380, 1985.

Schulz, M., Y. J. Balkanski, W. Guelle, and F. Dulac, Role of aerosol size distribution and source location in a three-dimensional simulation of a Saharan dust episode tested against satellite-derived optical thickness, *J. Geophys. Res.*, *103*, 10,579–10,592, 1998.

Servant, M., and S. Servant, Les formations lacustres et les diatomées du Quaternaire recent du fond de la cuvette tchadienne, *Rev. Geogr. Phys. Geol. Dyn.*, *13*(2), 6–76, 1970.

Shao, Y., and L. M. Leslie, Wind erosion prediction over the Australian continent, *J. Geophys. Res.*, *102*, 30,091–30,106, 1997.

Sokolik, I. N., and O. B. Toon, Incorporation of mineralogical composition into models of the radiative properties of mineral aerosol from UV to IR wavelengths, *J. Geophys. Res.*, *104*, 9423–9444, 1999.

Sokolik, I. N., D. M. Winker, G. Bergametti, D. A. Gillette, G.

Carmichael, Y. Kaufman, L. Gomes, L. Schuetz, and J. E. Penner, Introduction to special section: Outstanding problems in quantifying the radiative impacts of mineral dust, *J. Geophys. Res.*, *106*, 18,015–18,028, 2001.

Stone, R., Coming to grips with the Aral Sea's grim legacy, *Science*, *284*, 30–33, 1999.

Strain, P., and F. Engle (Eds.), *Looking at Earth*, 304 pp., Turner, Atlanta, Ga., 1996.

Swap, R., M. Garstang, S. Greco, R. Talbot, and P. Kallberg, Sahara dust in the Amazon basin, *Tellus, Ser. B*, *44*, 133–149, 1992.

Tegen, I., and I. Fung, Contribution to the atmospheric mineral aerosol load from land surface modification, *J. Geophys. Res.*, *100*, 18,707–18,726, 1995.

Tegen, I., and R. Miller, A general circulation model study of the inter-annual variability of soil dust aerosol, *J. Geophys. Res.*, *103*, 25,975–25,995, 1998.

Tegen, I., A. A. Lacis, and I. Fung, The influence on climate forcing of mineral aerosols from disturbed soils, *Nature*, *380*, 419–422, 1996.

Tegen, I., P. Hollrig, M. Chin, I. Fung, D. Jacob, and J. Penner, Contribution of different aerosol species to the global aerosol extinction optical thickness: Estimates from model results, *J. Geophys. Res.*, *102*, 23,895–23,916, 1997.

Thomas, D. S. G., and N. J. Middleton (Eds.), *Desertification: Exploding the Myth*, 194 pp., John Wiley, New York, 1994.

Thomas, J. V., S. N. Rajaguru, A. K. Singhvi, A. Kar, A. J. Kailath, and N. Juyal, Late Pleistocene-Holocene history of aeolian accumulation in the Thar Desert, India, *Z. Geomorphol. Supp.*, *116*, 181–194, 1999.

Tindale, N. W., and P. P. Pease, Aerosols over the Arabian Sea: Atmospheric transport pathways and concentrations of dust and sea salt, *Deep Sea Res.*, *46*, 1577–1595, 1999.

Torres, O., P. K. Bhartia, J. R. Herman, Z. Ahmad, and J. Gleason, Derivation of aerosol properties from a satellite measurements of backscattered ultraviolet radiation: Theoretical basis, *J. Geophys. Res.*, *103*, 17,099–17,110, 1998.

Torres, O., P. K. Bhartia, J. R. Herman, A Sinyuk, P. Ginoux, and B. Holben, A long-term record of aerosol optical depth from TOMS observations and comparison to AERONET measurements, *J. Atmos. Sci.*, *59*, 398–413, 2002.

Tripathi, J. K., and V. Rajmani, Geochemistry of the loessic sediments on Delhi Ridge, eastern Thar Desert, Rajasthan: Implications for exogenic processes, *Chem. Geol.*, *155*, 265–278, 1999.

Uematsu, M., Distribution and characterization of Asian aerosols over the western North Pacific region, *Global Environ. Res.*, *2*, 39–45, 1998.

Varushchenko, A. N., S. A. Lukyanova, G. D. Solovieva, A. N. Kosarev, and A. V. Kurayev, Evolution of the Gulf of Kara-Bogaz-Gol in the past century, in *Dynamic Earth Environments: Remote Sensing Observations from Shuttle-Mir Missions*, edited by K. P. Lulla and L. V. Dessinov, pp. 201–210, John Wiley, New York, 2000.

Volkel, J., and J. Grunert, To the problem of dune formation and dune weathering during the late Pleistocene and Holocene in the southern Sahara and Sahel, *Z. Geomorphol.*, *34*, 1–17, 1990.

Wurzler, S., T. G. Reisin, and Z. Levin, Modification of mineral dust particles by cloud processing and subsequent effects on drop size distributions, *J. Geophys. Res.*, *105*, 4501–4512, 2000.

Xuan, J., G. Liu, and K. Du, Dust emission inventory in northern China, *Atmos. Environ.*, *34*, 4565–4570, 2000.

Yaalon, D. H., Saharan dust and desert loess: Effect on surrounding soils, *J. Afr. Earth Sci.*, *6*, 569–571, 1987.

Yung, Y. L., T. Lee, C.-H. Wang, and Y.-T. Shieh, Dust: A diagnostic of the hydrologic cycle during the Last Glacial Maximum, *Science*, *271*, 962–963, 1996.

Zhang, X. Y, R. Arimoto, Z. An, and S. Zhi, Dust emission from Chinese desert sources linked to variations in atmospheric circulation, *J. Geophys. Res.*, *102*, 28,041–28,047, 1997.

T. E. Gill, Department of Civil Engineering, Texas Tech University, P.O. Box 42101, Lubbock, TX 79409-2101, USA. (tom.gill@ttu.edu)

P. Ginoux, Goddard Space Flight Center, Georgia Institute of Technology, Greenbelt, MD 20771, USA. (ginoux@rondo.gsfc.nasa.gov)

S. E. Nicholson, Department of Meteorology, Florida State University, Tallahassee, FL 32306-3034, USA. (sen@huey.met.fsu.edu)

J. M. Prospero, Rosenstiel School of Marine and Atmospheric Science, University of Miami, 4600 Rickenbacker Causeway, Miami, FL 33149-1098, USA. (jprospero@rsmas.miami.edu)

O. Torres, Joint Center for Earth Systems Technology, University of Maryland, Baltimore County, Baltimore, MD 21250, USA. (torres@tparty.gsfc.nasa.gov)